Published in final edited form as:
J Neurosci. 2009 April 8; 29(14): 4392–4407. doi:10.1523/JNEUROSCI.5609-08.2009.

Interaction of stimulus-driven reorienting and expectation in ventral and dorsal fronto-parietal and basal ganglia-cortical networks

Gordon L. Shulman[1], **Serguei V. Astafiev**[2], **Danny Franke**[2], **Daniel L. W. Pope**[1], **Abraham Z. Snyder**[2], **Mark P. McAvoy**[2], and **Maurizio Corbetta**[1,2,3]

[1]Department of Neurology, Washington University, St. Louis, MO 63110

[2]Department of Radiology, Washington University, St. Louis, MO 63110

[3]Department of Anatomy and Neurobiology, Washington University, St. Louis, MO 63110

Abstract

Shifts of attention to unattended stimuli (stimulus-driven reorienting) are often studied by measuring responses to unexpected stimuli, confounding reorienting and expectation. We separately measured the blood-oxygenation-level-dependent (BOLD) signal for both factors by manipulating the probability of salient visual cues that either shifted attention away from or maintained attention on a stream of visual stimuli. The results distinguished three networks recruited by reorienting.

Right temporo-parietal junction (TPJ), the posterior core of a ventral fronto-parietal network, was activated more by cues for shifting than maintaining attention independently of cue location and probability, acting as a switch. TPJ was separately modulated by low probability cues, which signaled a breach of spatial expectation, independently of whether they shifted attention. Under resting conditions, TPJ activity was correlated (resting-state functional connectivity MRI, (rs-fcMRI)) with right inferior frontal gyrus (IFG), an anterior component of the ventral network. Nevertheless, IFG was activated only by unexpected shifts of attention, dissociating its function from TPJ. Basal ganglia and frontal/insula regions also were activated only when reorienting was unexpected but showed strong rs-fcMRI among themselves, not with TPJ/IFG, defining a distinct network that may retrieve/activate commands for shifting attention.

Within dorsal fronto-parietal regions, shifting attention produced sustained spatially-selective modulations in intraparietal sulcus (IPS) and FEF, and transient less selective modulations in precuneus and FEF. Modulations were observed even when reorienting was likely, but increased when reorienting was unexpected. The latter result may partly reflect interactions with lateral prefrontal components of the basal-ganglia/frontal/insula network that showed significant rs-fcMRI with the dorsal network.

Keywords

attention; fMRI; executive; connectivity; globus pallidus; frontal; parietal; vision

Corresponding Author: Gordon L. Shulman, Dept. of Neurology, Box 8111, 4525 Scott Ave, rm 2109, St. Louis, MO 63110, Tel: 314-362-8880, Fax: 314-362-6911, E-mail: gordon@npg.wustl.edu .
Author Addresses: Serguei Astafiev, Abraham Snyder, Danny Franke, Mark McAvoy, Dept. of Radiology, Box 8225, 4525 Scott Ave, St. Louis, MO 63110
Maurizio Corbetta, Daniel Pope, Dept. of Neurology, Box 8111, 4525 Scott Ave, St. Louis, MO 63110

Introduction

Survival can depend on quickly responding to behaviorally important objects that appear outside the focus of attention, a process here called stimulus-driven reorienting (Corbetta and Shulman, 2002). Because important unattended objects are often unexpected, however, understanding the function of neural systems during stimulus-driven reorienting requires a knowledge of how those systems are modulated by both shifts of attention and the likelihood of shifting attention. Unfortunately, previous studies have largely confounded these factors.

Stimulus-driven reorienting has often been studied using 'oddball' (Marois et al., 2000) and Posner cueing paradigms (Arrington et al., 2000; Corbetta et al., 2000; Macaluso et al., 2002), which ensure that targets are unattended by making them unexpected. Larger BOLD responses to unexpected/unattended targets are consistently reported in R TPJ and R VFC, whose activity is highly correlated in the resting state (Fox et al., 2006), supporting proposals that they form a ventral attention network for stimulus-driven reorienting (Corbetta et al., 2008).

Previous studies have not identified separate roles for TPJ and VFC, but these regions may be dissociated when reorienting and expectation are factorially manipulated. Prefrontal regions may be recruited only when reorienting is unexpected and greater cognitive control is required (Fuster, 1989; Miller and Cohen, 2001). Under these conditions, commands to shift attention may be retrieved/activated in working memory and motor responses prepared under the current set may be inhibited (Nobre et al., 1999). In contrast, TPJ may be recruited whenever reorienting occurs, functioning as a reset mechanism that promotes the reorganization of task networks (Corbetta et al., 2008).

Phasic dopaminergic inputs to striatum (Schultz, 1998) have also been proposed to facilitate shifts of attention to unexpected, behaviorally important stimuli (Redgrave et al., 1999a, b; Horvitz, 2000; Zink et al., 2006). Accordingly, striatum is activated more by shifts of attention to infrequent than frequent peripheral stimuli (Zink et al., 2003). We manipulated both reorienting and the frequency of reorienting rather than frequency alone to determine whether basal ganglia showed an interaction pattern similar to that discussed above for prefrontal regions, possibly defining a role for cortical-basal ganglia loops (Alexander et al., 1986) in stimulus-driven reorienting.

While the ventral attention network is activated by stimulus-driven reorienting to important stimuli, a dorsal fronto-parietal network is activated by orienting irrespective of whether stimuli are present or absent (Kastner and Ungerleider, 2000; Corbetta and Shulman, 2002). This network likely implements the complex computations for shifting attention, sending biasing signals to sensory regions (Desimone and Duncan, 1995; Bisley and Goldberg, 2003; Moore and Armstrong, 2003; Ruff et al., 2006; Bressler et al., 2008). Because of their central role in shifting attention, dorsal fronto-parietal regions should be activated even when reorienting is expected, but activations may increase when reorienting is unexpected and commands to shift attention must be assembled.

We evaluated the above hypotheses by factorially manipulating shifting/maintaining attention to stimuli and the likelihood of shifting/maintaining attention, and measured the resulting BOLD signals in ventral and dorsal attention networks, basal ganglia, and prefrontal regions.

Methods

Paradigm

Throughout the paper, the term stimulus-driven reorienting is used to refer to shifts of attention evoked by cues presented outside the current focus of attention. Stimulus-driven reorienting can potentially involve both goal-driven and automatic (i.e. exogenous) components of reorienting, the latter isolated by measuring shifts of attention evoked by salient but non-informative or task-irrelevant cues (Posner and Cohen, 1984). However, previous studies have shown that TPJ activation during stimulus-driven reorienting primarily reflects goal-driven rather than exogenous shifts of attention ((Downar et al., 2001; de Fockert et al., 2004; Kincade et al., 2005; Serences et al., 2005; Indovina and Macaluso, 2007); see (Corbetta et al., 2008) for review). Therefore, we do not use the term stimulus-driven reorienting to refer to automatic shifts of attention but more generally to refer to shifts of attention to stimuli outside the current focus of attention.

We manipulated the probability of cues that shifted attention or maintained attention at the current location within a factorial design, and measured the resulting blood-oxygenation-level-dependent (BOLD) signals. Subjects searched for a target object in two task-relevant rapid-serial-visual-presentation (RSVP) streams, one left and one right of fixation (see Figure 1). Each stream was flanked by three irrelevant distracter RSVP streams in order to increase the need for careful spatial selection. A salient, easily detectable cue stimulus (a filled red square) presented without accompanying objects in one of the task-relevant RSVP streams indicated which of the two streams contained the target. The cue was presented multiple times over a block. A cue might occur in the same stream as the previous cue, indicating that subjects should continue to monitor the same stream (a ‘stay’ cue) or it might occur in the opposite, unattended stream, indicating that subjects should shift their attention to the new stream (a ‘shift’ cue). Target identification was set at difficult levels (see below). The high difficulty of the target discrimination and the presence of distracter streams, coupled with the high salience of the cue stimulus, encouraged subjects to attend closely to the cued stream rather than distributing attention across both streams. In one set of scans, a cue was highly likely to occur in the same stream as the previous cue (i.e. the probability that the cue was a stay cue was 0.86), in another set of scans, a cue was highly likely to occur in a different stream than the previous cue (i.e. the probability that the cue was a shift cue was 0.86), while in a third set, stay and shift cues were equally likely. This design, a modification of earlier stay/shift paradigms (Yantis et al., 2002) in which symbolic cues at the current location of attention instructed ‘stay’ or ‘shift’, allowed a factorial manipulation of stimulus-driven reorienting and expectation.

The experimental design controlled for several processes that are separate from stimulus-driven reorienting, in addition to expectation. Activations were measured to a cue that indicated where but not when a target would appear, eliminating time-locked activations related to temporal prediction of target onset (Coull and Nobre, 1998; Coull et al., 2000), including those involving a heightened state of alertness or motor preparation. Secondly, activations were measured to cues rather than to targets requiring a detection response. When a target detection response is overt, time-locked activations may occur that are related to response selection, response execution, performance monitoring, and the interaction of these processes with expectation (e.g. selecting/executing an unexpected as compared to an expected stimulus-response mapping likely increases activations in some areas). When a detection response is covert, such as counting, time-locked activations may occur related to the covert process (e.g. incrementing a counter and maintaining it in working memory), performance monitoring, and the interaction of these processes with expectation. The present experimental design isolated effects of reorienting and expectation that were separate from these target- and response-related processes.

Subjects and stimuli

Thirty-five right-handed subjects gave informed consent in accordance with guidelines set by the Human Studies Committee of Washington University. 24 subjects participated in the RSVP experiment, but data was eliminated from two subjects due to eye movements and one subject due to movement artifacts. 11 subjects participated in the resting-state connectivity experiment.

Stimuli were presented with a Power Macintosh G4 computer (Apple, Cuperino, CA) using Matlab software (Mathworks, Natick, MA) with the psychophysics toolbox (Brainard, 1997; Pelli, 1997). Images were projected to the head of the bore of the scanner via an LCD projector (Sharp LCD C20X) and viewed with a mirror attached to the head coil.

Four RSVP streams of colored drawings of inanimate objects were presented in the left visual field and four in the right visual field (Figure 1). The target streams, which could potentially contain the target object, were surrounded by three non-target streams that contained only distracter objects. One non-target stream was positioned above the target stream, one was below, and a third was more eccentric. The target streams were located at an eccentricity of 5 deg. All objects in both target and non-target streams were roughly 3 deg by 3 deg. Distracter objects were sampled from a population of 40 objects and target objects were sampled from a separate population of 12 objects. The cue was a filled red square, 3 deg by 3 deg, located in the target stream. None of the objects were red and when the cue was presented, no other objects were present in the field.

The discriminability of the target object was adjusted by adding colored noise to each object in the target streams in both fields (i.e. noise was added to both potential target streams, not only to the stream that was presently cued). To create the noise, a percentage of the pixels defining the target stream location in each field were randomly colored, with each pixel displayed in one of five randomly selected hues.

Procedure

Subjects were shown the target object, randomly selected from the twelve objects designated as targets, prior to each scan. The target object for a scan never appeared as a non-target object in another scan. At the start of a scan, subjects fixated a central cross for 41.2 seconds. A cue then appeared at one of the two target stream locations, indicating the initial stream to be attended. The eight RSVP streams then appeared. Each display frame of 8 objects was presented for 120 msec, with no interstimulus interval (ISI) separating it from the next frame. Each cue appeared for 160 msec, again with a 0 msec ISI before the next display frame. Subjects pressed an MR compatible button when they detected a target. Target objects only appeared in the cued stream. A target occurred with a fixed probability independently in each 1.08 sec interval such that on average a target occurred about once every 10.5 seconds. To allow separate button presses to be recorded for each target, the minimum inter-target interval was restricted to 1 sec. Cues occurred on average every 2.06, 4.12, or 6.18 seconds within a temporal window of plus or minus 400 msec centered on those values. Cue onset and target onset were independent except that a target could not occur simultaneously with a cue or in the 120 msec display frame preceding a cue. Therefore, cues provided spatial information about targets but essentially no temporal information. Following the initial 41.2 sec fixation period, the stimulus display was presented for 185.4 secs and was followed by a 30.9 sec fixation period, resulting in a scan duration of 257.5 secs.

Each subject received 16 scans. In six scans the probability of a stay cue was 0.14 (shift cue probability was 0.86), in four scans, stay cue probability was 0.5 (shift cue probability, 0.5) and in six scans stay cue probability was 0.86 (shift cue probability, 0.14). Subjects were

informed prior to each scan that it was ‘mostly stay’, ‘mostly shift’, or ‘stay and shift equally likely’.

Prior to the scanning session, each subject received a practice session in which the noise level (percentage of voxels randomly colored) was determined at which the task could be performed with a 60% target hit rate. This fraction was then decreased by 0.05 for the session in the scanner, since our experience was that subject performance was slightly worse in the scanner. During the scanning session, the fraction was occasionally varied for each subject in order to roughly maintain performance at a desired level, using the following rules: if %hits < 10 on a scan, the noise fraction was lowered by .1; if %hits < 40 on two consecutive scans, the noise was lowered by .1; if %hits < 50 on three consecutive scans, the noise was lowered by .05; if %hits > 90 on a scan, the noise fraction was raised by .05; if %hits > 80 on two consecutive scans, the noise was raised by .05; if %hits > 70 on three consecutive scans, the noise was raised by .05.

Eye movement recording

To verify that subjects followed instructions to remain fixated, each subject’s eyes were carefully monitored via a camera on all scans. Moreover, eye movements were recorded for each subject using an infrared eye-tracking system on some scans during the scanner session (22 subjects, ISCAN ETL-200) or during a behavioral session outside of the scanner (2 subjects, ASL 504). Eye movement data was lost for one subject because of technical difficulties.

FMRI Methods

Image acquisition—MRI scans were collected on a Siemens Allegra 3T scanner, using an asymmetric spin-echo echoplanar imaging sequence to measure blood oxygenation-level-dependent (BOLD) contrast. 31 contiguous 4mm slices were acquired, 4 × 4 mm in-plane resolution, TE = 25 msec, flip angle = 90°, slice TR = 2.06 sec. Structural images included a sagittal MP-RAGE T1-weighted sequence (TR = 1810 ms, TE = 3.93 ms, flip angle = 12°, TI = 1200 ms, voxel size = 1×1×1.25 mm).

Preprocessing—Differences in the acquisition time of each slice in an MR frame were compensated by sinc interpolation so that all slices were aligned to the start of the frame. A whole-brain normalization corrected for changes in signal intensity across scans. Data were realigned within and across scans to correct for head movement. Images were resampled into 3-mm isotropic voxels and warped into a standardized atlas space (Talairach and Tournoux, 1988). The resampling required for movement correction and atlas transformation was performed in the same step to minimize sampling noise.

Statistical analysis—The BOLD signal during the 185.6 sec task period was analyzed with the general linear model (GLM). Four cue regressors (stay left, stay right, shift left, and shift right), each consisting of 10 separate timepoint regressors that estimated the hemodynamic response out to 18.5 seconds without assuming a response shape (Ollinger et al., 2001), were estimated for each probability condition (i.e. stay cue probability = 0.14, 0.50, and 0.86). Four sets of target timepoint regressors, not separated by cue probability, were also estimated: detected target left and right, missed target left and right. In addition, regressors were included for baseline, linear trend and low frequency components (<.009 Hz) of the BOLD signal in each scan.

The resulting whole-brain maps of timecourses for cues and targets were smoothed by a Gaussian filter with a full-width-at-half-maximum of 6 mm and analyzed by ANOVAs in which subject was treated as a random effect. All voxel-wise ANOVAs were corrected for non-

independence of time points by adjusting the degrees of freedom and corrected over the brain for multiple comparisons using joint z-score/cluster size thresholds (Forman et al., 1995) corresponding to z=3.0 and a cluster size of 13 face-contiguous voxels. The z-score/cluster size thresholds were determined using volume-based monte-carlo simulations. Regional ANOVAs were conducted on regions-of-interest (ROIs) that were automatically created from the voxel-level maps using a peak-finding routine (Kerr et al., 2004). For each subject and ROI, the BOLD timecourses for a condition were averaged over all voxels in the ROI, and the regional timecourse for each condition was entered into an ANOVA, which corrected for non-independence of time points by adjusting the degrees of freedom. A significance threshold of $p<.01$, uncorrected for the number of tested ROIs, was adopted for regional analyses. For display purposes, volumes were mapped to surface-based representations using the PALS atlas and CARET software (Van Essen, 2005).

Resting state functional connectivity MRI

In order to determine whether regions that showed specific task modulations formed consistent networks, resting-state functional connectivity MRI (rs-fcMRI) of the task-evoked foci in these regions were evaluated in an independent group of 11 subjects. Rs-fcMRI assesses the temporal correlation between BOLD timeseries in different regions under conditions in which subjects are lying at rest with no experimenter-imposed task. Regions that are co-activated in task activation studies of attention show strong rs-fcMRI (Fox et al., 2006), replicating the putative dorsal and ventral attention networks (Corbetta and Shulman, 2002). Therefore, rs-fcMRI measures the degree to which regions form coherent networks in the resting state.

Rs-fcMRI maps were computed using previously published methods (Fox et al., 2006; He et al., 2007). Each subject received six 264 sec BOLD scans (aside from one subject, whose scan duration was 328 sec, and another subject who received only 4 264 sec scans) in which fixation was maintained on a central plus sign in an otherwise empty field. Several pre-processing steps were conducted on the BOLD timeseries in addition to those described above: 1) temporal filtering that retained frequencies in the 0.009–0.08 Hz band and 2) removal by linear regression of i) six parameters obtained by correction of head motion, ii) the signal averaged over the whole brain, excluding the ventricles iii) the signal over a ventricular region, and iv) the signal from a white matter region. Temporal derivatives of these regressors were also included in the linear model, accounting for time-shifted versions of spurious variance.

Voxel-wise analyses—A voxel-wise map was computed for a single ‘seed’ ROI, which was either a 6 mm (cortical regions) or 3 mm (basal ganglia) radius sphere centered at a particular Talairach coordinate, indicating the correlation of each voxel in the brain with the indicated ROI. A smaller ‘seed’ ROI was used for basal ganglia to avoid contributions from adjacent structures. The BOLD time series was averaged over all voxels in the seed ROI, the voxel-wise pearson correlation coefficients between that ROI and all other voxels were computed, and the Fisher z-transform was applied. For a group statistical analysis of the voxel-wise map, a 1-sample t-test with subject as a random-effect was computed on the Fisher z-transformed values and corrected for multiple comparisons using a z-score threshold of z=3.0 and a cluster size of 17 face-contiguous voxels.

Regional analyses—The significance of rs-fcMRI between two regions or ROIs was computed as follows. For each subject, the voxels within each ROI were averaged and a regional timecourse was computed. Then the correlation coefficient between the two regional timecourses was computed and the Fisher z-transform was applied. Finally, a random-effects 1-sample t-test was performed on the Fisher z-transformed values from the individual subjects. A significance threshold of $p<.01$ was adopted for regional analyses, uncorrected for the number of ROI pairs that were tested. In addition to pairwise analyses, we also computed the

average rs-fcMRI within sets of regions by averaging within each subject the Fisher z-transformed value for each ROI-ROI pair within the set. Similarly, we measured the rs-fcMRI between sets of regions by averaging the Fisher z-transformed values for all ROI-ROI pairs between sets, where each ROI in a pair comes from a different set.

Results

Behavior

Subjects detected on average 61.7% of targets, with a mean false alarm rate (# false alarms/# targets) of 4.7%. The detection rate was well below ceiling, indicating that the task was quite difficult, but also well above the false alarm rate, indicating above chance performance. Mean correct reaction time (RT) was 596 msec.

An ANOVA on percent detection rates with Cue Probability (i.e. probability of the cue immediately preceding the target: 0.14, 0.50, 0.86) and Cue Type (i.e. type of cue immediately preceding the target: stay, shift) as factors indicated no significant effect of Cue Probability ($F(2,40) = 1.77$), Target Type ($F(1,20) = .37$, ns), or Cue Probability by Cue Type interaction ($F(2,40) = 1.71$, ns). A similar ANOVA on RTs also yielded no effects: Cue Probability ($F(2,40) = 1.06$), Cue Type ($F(1,20) = .70$, ns), Cue Probability by Cue Type interaction ($F(2,40) = 1.50$, ns). These results indicate that attention to the cued stream was similar across conditions and that subjects did not prematurely shift attention to an uncued stream when shift cues were likely.

fMRI

For each set of regions thought to be involved in stimulus-driven reorienting, i.e. TPJ, frontal cortex and basal ganglia, and dorsal fronto-parietal cortex, we examine the BOLD activations due to stimulus-driven reorienting, defined by significant differences between stay and shift cues, and then describe how those activations were modulated by expectation.

Results for R TPJ

Modulations due to stimulus-driven reorienting—R TPJ was activated by stimulus-driven reorienting. The left coronal slice in Figure 2A displays voxels in R TPJ that showed significantly different timecourses following shift and stay cues (i.e. voxels that showed a significant interaction of Cue Type (shift, stay) by Time (10 time points). All voxel-wise ANOVAs were corrected for multiple comparisons over the whole brain (see methods)). A strong activation was observed in R TPJ (52, −49, 17; z=6.45), which extended dorsally into the supramarginal gyrus (51, −45, 32; z=5.62). No significant activations were observed in L TPJ, consistent with the right hemisphere dominance that has previously been observed for this region during stimulus-driven reorienting (Corbetta and Shulman, 2002).

R TPJ activations during reorienting did not depend on the location of the cue, confirming previous results (Corbetta et al., 2000). A regional ANOVA conducted on the R TPJ ROI formed from the shift vs. stay activation (i.e. the Cue Type by Time map) indicated no significant interaction of Cue Type by Cue Location (left, right) by Time ($F(9, 180) = .67$). The voxel-wise map for the Cue Type by Cue Location by Time interaction also showed no effects in R TPJ. The timecourse of R TPJ activation, shown in the leftmost graph of Figure 2, indicated a transient response to a shift cue, relative to a stay cue, at both cue locations.

A difference between shift and stay cues was observed even when they were both highly likely. A voxel-wise ANOVA, conducted on just the stay and shift cue data from the p=0.86 conditions yielded a significant Cue Type by Time activation in R TPJ (50, R̂49, 14, z=4.88), as shown in Figure 2A.

Modulations due to expectation—R TPJ activity was affected by cue probability in addition to stimulus-driven reorienting. A regional ANOVA confirmed that the R TPJ ROI formed from the shift vs. stay activation showed a significant interaction of Cue Probability (0.14, 0.50, 0.86) by Time ($F(18, 360) = 3.91$, $p<.0001$). Moreover, the voxel-wise map for the interaction of Cue Probability by Time included a significant activation in R TPJ (47, −48, 17; z=5.18), shown in the coronal slice in Figure 2B, that was contained within the TPJ component of the more extensive shift vs. stay activation. However, the cue probability and shift vs stay effects did not interact, i.e. were additive. A regional ANOVA on the shift vs. stay ROI in R TPJ indicated no higher-order interaction of Cue Probability by Cue Type by Time ($F(18, 360) = .19$), and no higher-order interaction was observed for R TPJ in the voxel-wise map of the interaction.

Bolstering the evidence for separate reorienting and probability signals, R TPJ showed significant effects of cue probability even when the cue did not evoke a shift of attention. An analysis of the effect of cue probability in just the stay cue condition identified a significant voxel-wise activation in R TPJ (47, −52, 14; z=3.75), and a significant effect in a regional ANOVA on the R TPJ ROI defined from the shift vs stay activation ($F(18, 360) = 2.06$, $p = .01$).

The timecourse of R TPJ activation as a function of cue type and probability is shown in the right graph in Figure 2. Low probability cues (red symbols) produced larger activations than middle or high probability cues (green and black symbols) irrespective of whether the cues signaled stay (open symbols) or shift (filled symbols). Notably, TPJ activity did not change linearly as a function of cue probability, with very similar responses for the medium and high probability cues (i.e. green and black symbols). This pattern indicates that R TPJ was activated when an expectation concerning the cue was breached, as in the low probability condition. A strong expectation was not present in the 0.50 condition, since stay and shift cues were equally likely, while the expectation in the 0.86 condition was confirmed rather than violated, leading to equivalent and lower activity in the latter two conditions. Voxel-wise ANOVAs in which the cue probability factor was confined to the 0.14 and 0.50 conditions or to the 0.50 and 0.86 conditions confirmed that R TPJ was significantly activated by the former comparison (46, −51, 16, z=3.93) but not by the latter. Finally, the timecourses supported the earlier conclusion that the reorienting and breach of expectation effects were additive. The BOLD signal in R TPJ was reasonably described by increments due to reorienting (shift 50, shift 86), breached expectation (stay 14), or their sum (shift 14).

To summarize, R TPJ showed significant effects of stimulus-driven reorienting to either visual field even when shifts of attention were likely and frequently performed, and these activations were not increased when reorienting was unlikely. R TPJ was independently (additively) activated by low probability cues, indicating separate signals for reorienting and breaches of expectation. R TPJ activations to unexpected targets in previous studies reflected a sum of reorienting and breach of expectation signals (Arrington et al., 2000; Corbetta et al., 2000; Marois et al., 2000; Macaluso et al., 2002).

Results for frontal/insula cortex and basal ganglia

Interaction of expectation and stimulus-driven reorienting—In contrast to R TPJ, several regions in frontal and insula cortex and basal ganglia (Figures 3A and 3B) were primarily activated by unexpected shift cues, resulting in a strong interaction of stimulus-driven reorienting and cue probability (see Table 1 for z-scores and coordinates of significant foci). Significant interactions in the voxel-wise map for Cue Probability by Cue Type by Time were observed in left anterior insula, anterior cingulate, and left dorsolateral prefrontal cortex (DLPFC) (Figure 3A), and in basal ganglia (Figure 3B), including bilateral dorsomedial globus pallidus and nearby regions in caudate, and right ventral striatum.

The timecourses of the frontal, insula, and basal ganglia responses (Figures 3A and 3B) were quite different than those for R TPJ. Low probability shift cues produced a time-locked response that was sometimes extended, but low probability stay cues and high probability shift cues evoked no activity. Therefore, these regions did not respond to unexpected cues that did not reorient attention, or to expected cues that evoked stimulus-driven shifts of attention. Rather, they mainly responded to unexpected cues that evoked a shift of attention. This interaction pattern was consistent with that expected for control regions that activate new attentional sets or inhibit competing processes (Fuster, 1989; Miller and Cohen, 2001). Anterior insula and anterior cingulate have been identified as the regions most consistently involved in cognitive control across a variety of tasks in human neuroimaging studies (Dosenbach et al., 2006).

A prior study demonstrated that greater activity in striatum was produced by infrequent than frequent randomly located peripheral stimuli that evoked shifts of attention (Zink et al., 2003), but did not test for an interaction of frequency and reorienting. Interestingly, this study manipulated expectation about temporal onset (i.e. infrequent stimuli were less expected), holding constant expectations about the spatial location of the peripheral stimulus. Here, the temporal predictability of cue onset was held constant across conditions (i.e. in all scans a cue appeared roughly every 2 to 6 seconds) and expectations about spatial location were varied.

In addition to the basal ganglia/frontal/insula circuitry defined by the interaction of stimulus-driven reorienting and expectation signals, we were interested in evaluating R VFC, the frontal core of the putative ventral attention network. VFC includes a collection of regions in R anterior insula, R IFG, and R MFG, which tend to be variably recruited in different experiments (Corbetta and Shulman, 2002). Of these regions, only R IFG showed an interaction of cue probability and stimulus-driven reorienting (Figure 3A), similar to the basal ganglia/frontal/insula regions discussed above, although the timecourse of BOLD activity was noisier. While activations were again mainly observed in the low probability shift cue condition, the transient and time-locked nature of the activation was less clear. However, the response in this region was quite different than that observed in R TPJ. The resting-state connectivity results presented below provide strong evidence that the present R IFG focus falls within the ventral network.

To summarize, basal ganglia and prefrontal/insula regions were only activated by stimulus-driven shifts of attention that were unexpected. Neither a breach of spatial expectation (i.e. spatial prediction error) nor reorienting alone was sufficient to activate these regions.

Results for dorsal fronto-parietal cortex

Dorsal fronto-parietal regions are thought to play a primary role in controlling attention (Corbetta et al., 1993; Nobre et al., 1997; Vandenberghe et al., 1997; Kastner et al., 1999; Hopfinger et al., 2000; Corbetta et al., 2002; Sylvester et al., 2007). We first identify two types of signals that were evoked by stimulus-driven reorienting - a transient signal that showed relatively weak spatial selectivity and a sustained signal that showed strong selectivity - and then examine how those signals for reorienting were affected by expectation.

Transient modulations due to reorienting in precuneus and parts of FEF/precentral—Large regions within dorsal fronto-parietal cortex showed transient responses that differed for shift and stay cues, averaged over cue location, as indicated in Figure 4A, which shows the voxel-wise Cue Type (shift, stay) by Time ANOVA map. Parietal activations were observed most robustly in bilateral precuneus, extending into superior parietal lobule (SPL), and to a lesser degree in bilateral intraparietal sulcus (IPS) extending into postcentral sulcus (see Table 2). Significant dorsal frontal activations were observed most robustly in bilateral human frontal-eye field (FEF), extending laterally and ventrally in bilateral precentral sulcus, and in SMA. The graphs in Figure 4A, which show timecourses for the four regions in

dorsal fronto-parietal cortex with the highest z-scores for the shift vs stay effect (Table 2), indicate the transient character of the bilateral precuneus/SPL and L FEF responses, which resembled a 'shift' signal (Serences and Yantis, 2006a), as previously reported for these regions during symbolically-directed shifts of attention (Yantis et al., 2002; Kelley et al., 2007).

Three of the four ROIs shown in Figure 4A did not show significant spatial selectivity in regional ANOVAs, matching a previous report (Yantis et al., 2002). However, this result should be treated cautiously. Spatially selective signals have been reported in precuneus (Hagler et al., 2007; Jack et al., 2007; Sylvester et al., 2007; Saygin and Sereno, 2008) and both L FEF and L precuneus/SPL ROIs showed the expected trend for greater contralateral activity, a trend that was significant in a regional ANOVA on the R FEF ROI (Cue Type by Cue Location (left, right) by Time ($F(9,180)=2.70$, $p=.0095$)). Spatially selective signals may be easier to image when the underlying neural processes are sustained (e.g. maintenance of attention) rather than transient (e.g. shifts of attention), as shown in the next section.

Sustained, spatially-selective modulations in IPS and parts of FEF/Precentral— Regions in IPS and parts of FEF/Precentral sulcus showed sustained BOLD responses in which the difference between stay and shift cues significantly depended on whether the cue was contralateral or ipsilateral, as shown in Figure 4B by the voxel-wise ANOVA map for Cue Location (left, right) by Cue Type (shift, stay) by Time (Table 2). Highly significant, spatially-selective responses were also observed throughout occipital cortex (e.g. lateral view in Figure 4B and Supplementary Figure 1). Because the ANOVA compared stay and shift cues that were presented at the same location, controlling for purely sensory activations, the activations reflected a spatially-selective attentional modulation. Previous studies have reported spatial selectivity in these regions (Sereno et al., 2001; Schluppeck et al., 2005; Silver et al., 2005; Hagler and Sereno, 2006; Serences and Yantis, 2006b; Jack et al., 2007; Molenberghs et al., 2007; Swisher et al., 2007).

The timecourses of the BOLD signal in dorsal IPS and FEF are shown in Figure 4B. Shift cues to a location produced a sustained increase in the contralateral hemisphere and a sustained decrease in the ipsilateral hemisphere that eventually returned to the level of activation produced by a stay cue, which showed smaller differences between ipsilateral and contralateral locations. The sustained decrease was not a true deactivation, however, since it did not occur relative to a resting baseline but only relative to a baseline that included both sensory-evoked and task-evoked activity; i.e. the important result was the difference between the ipsilateral and contralateral cue timecourses. The sustained nature of the timecourses likely reflected the maintenance of attention and/or the modulation of stimulus-evoked activity from the RSVP stream at the cued location.

While in parietal cortex there was a clear functional-anatomical segregation between the IPS regions that most strongly showed sustained signals and the precuneus regions that most strongly showed transient 'shift' signals, the functional-anatomical segregation between the two types of signals in FEF/precentral cortex was less clear and suggested some mixing of the two signal types (e.g. R FEF foci in Figures 4A and 4B).

Interaction of expectation and reorienting: regions showing transient signals— We next consider how expectation affected reorienting in dorsal fronto-parietal regions that showed transient 'shift' signals. Figure 5A, which shows timecourses for the four ROIs showing the largest shift vs. stay z-scores, indicates that activations were greater for low probability than middle or high probability cues. The latter two conditions showed similar activation magnitudes, again indicating that the effect of cue probability was best described as a breach of expectation. Importantly, however, the probability effect was largely confined to

shift cues, with weak or absent effects for stay cues, unlike the additive effects of probability and reorienting observed in R TPJ.

The interaction of reorienting and expectation was significant in both of the medial parietal regions showing transient spatially non-selective shift signals, i.e. R precuneus (6, −56, 54, F (18, 360) = 2.17, p=.01) and L precuneus/SPL (−12, −58, 55, F(18, 360) = 2.29, p=.006), and was marginally significant in R FEF (25, −9, 54, F(18, 360) = 1.81, p=.039). These regional analyses were corroborated by voxel-wise results shown in Supplementary Figure 2 and Table 2. Finally, the same two medial parietal ROIs that showed a significantly greater effect of shifting attention when cues were unexpected, nevertheless showed highly significant shift vs stay differences in regional analyses when only expected (high probability) cues were analyzed (L precuneus/SPL: −12, −58, 55: F(9,180) = 4.99, p<.0001; R precuneus: 06, −56, 54: F(9,180) = 4.15, p<.0001) (see Supplementary Figure 2 and Supplementary Figure 3 for corresponding effects in the voxel-wise maps).

Interaction of expectation and reorienting: regions showing sustained, spatially-selective signals—Figure 5B shows the effect of expectation on the timecourse of activation following a shift cue in the four dorsal fronto-parietal regions from Figure 4B that showed sustained, spatially selective differences between stay and shift cues. Low probability shift cues increased the activation from both ipsilateral and contralateral cues, resulting in an effect of cue probability that was largely independent of spatial location and therefore did not enhance the spatial selectivity of the activation. While breaches of expectation produced overall increases in the BOLD signal, the interaction of expectation and reorienting was less robust. Regional ANOVAs on the four ROIs yielded a marginally significant Cue Type by Cue Probability by Time interaction in one parietal region, L IPS (−27, −58, 50, F(18,360) = 1.83, p=.036) and in R FEF (31, −12, 51, F(18, 360) = 1.74, p=.049), indicating that in some ROIs the probability effect modestly differed for stay and shift cues. The weaker nature of the effects of expectation on reorienting was also evident in the corresponding voxel-wise statistical map (Supplementary Figure 2), which was not significant in IPS.

To summarize, in dorsal fronto-parietal regions, breaches of expectations enhanced signals due to reorienting. This effect was more pronounced in medial parietal (precuneus) regions showing transient signals to the cue than in more lateral parietal regions (IPS) showing sustained spatially-selective signals, possibly reflecting different functional roles of these regions in shifting and maintaining attention, respectively. As with the basal ganglia/frontal/insula regions discussed above, interacting effects of expectation and reorienting cannot be ascribed to a general increase in arousal when an expectation is breached, but indicate a specific effect of expectation on shifts of attention. However, unlike basal ganglia/frontal/insula regions, dorsal fronto-parietal regions showed highly significant differences between stay and shift cues even when those cues were expected, consistent with the primary role of the dorsal network in shifting attention.

Interaction of expectation and reorienting across networks

The preceding analyses have indicated that R TPJ, basal ganglia/frontal/insula regions and dorsal fronto-parietal ‘shift’ regions fall along different points on a continuum that reflects the effect of expectation on reorienting. TPJ falls on one end of the continuum with equivalent shift vs stay activations under high and low probability conditions, the most robust dorsal fronto-parietal ‘shift’ regions fall in the middle, with shift vs stay activations that are present under high probability conditions but are increased under low probability conditions, and basal-ganglia/frontal/insula regions and R IFG fall on the other end, with shift vs stay activations only under low probability conditions.

We illustrate this point using a metric that allows the different regions to be more readily compared. The graph in Figure 6 displays a shift minus stay magnitude for each probability level, normalized by the magnitude at the 0.14 probability level, where a single line in the graph displays the magnitudes from a single region. Magnitudes were computed from the observed timecourses using a standard hemodynamic response function (Boynton et al., 1996). Figure 6 shows the normalized magnitudes for TPJ and SMG (from the Cue Type by Time map; Table 1, Figure 2), the 4 dorsal fronto-parietal regions that showed the largest z-scores for the difference between shift and stay cues (from the Cue Type by Time map; Table 2, Figure 4A) and the 8 IFG, frontal/insula and basal ganglia regions from the voxel-wise map for the interaction of Cue Type by Cue Probability by Time (Table 1, Figure 3). The distribution of the three region sets corresponded to the description above, with TPJ/SMG and basal ganglia/frontal/insula regions on the extremes and dorsal fronto-parietal 'shift' regions in the middle.

At the level of individual subjects, the normalized magnitude measure was very unstable and sensitive to noise since some subjects had small magnitudes in the denominator. Therefore, we used the non-parametric Mann-Whitney U-test to compare the group-averaged distributions between region sets at the 0.86 probability level normalized values, which by hypothesis should most strongly differentiate the three region sets. Significant differences were found between dorsal fronto-parietal cortex and basal ganglia/frontal/insula cortex (U=0, U`=32; p=.007) and basal ganglia/frontal/insula vs TPJ/SMG (U=0, U`=16, p=.037). The difference between dorsal fronto-parietal cortex vs TPJ/SMG was marginal (U=0, U`=8; p=.064), entirely because of the small number of regions involved (n=6). However, each of the 24 dorsal fronto-parietal ROIs listed in Table 2 from the Cue Type by Time and Cue Type by Cue Probability by Time voxel-wise maps had a value for the normalized 0.86 shift vs. stay magnitude that was less than that for either R SMG or R TPJ.

Resting-state functional connectivity

The task activation analyses indicated that three sets of brain regions were differentially modulated by reorienting and expectation. To determine if these regions formed coherent networks, we measured resting-state functional connectivity (rs-fcMRI), using the task-evoked foci as seeds, in an independent set of subjects (n=11).

Basal ganglia/frontal/insula—Figure 7A shows the rs-fcMRI maps that used as seeds the dorsal basal ganglia ROIs from the Cue Type by Cue Probability by Time interaction. A striking pattern of selective rs-fcMRI was observed with the task-evoked frontal/insula ROIs in anterior cingulate, L anterior insula, and L DLPFC that also showed the Cue Type by Cue Probability by Time interaction (indicated in Figure 7A by the white circles). Supplementary Figure 4 shows that strong inter-regional rs-fcMRI was obtained between the cortical regions of this network, namely L DLPFC (the more inferior focus), anterior cingulate, and L anterior insula. These observations from the voxel-wise maps were confirmed with pair-wise regional statistical analyses (see Supplementary Text for detailed statistics). As summarized in Table 3, rs-fcMRI for all of the ROI-ROI pairs within the basal ganglia/frontal/insula network exceeded the $p<.01$ significance threshold, except for a single pair with $p<.05$.

In summary, a robust basal-ganglia/frontal/insula resting-state network was observed in regions that were only activated by unexpected cues to shift attention. Interactions between human basal ganglia and frontal and insula cortex (Postuma and Dagher, 2006; Di Martino et al., 2008) are thought to be consistent with the principle of parallel cortico-striatal loops (Alexander et al., 1986; Alexander and Crutcher, 1990), although the disparate frontal/insula regions of the current network may not be subsumed within a single loop.

R TPJ/IFG—Previous reports have indicated that R IFG and R TPJ show strong functional connectivity (Fox et al., 2006; He et al., 2007), supporting the hypothesis of a ventral attention network. While in the present study R IFG and R TPJ showed different activation patterns, they nonetheless showed strong and selective rs-fcMRI in voxel-wise maps that used each focus as a seed (Figure 7B). A regional analysis confirmed highly significant rs-fcMRI between the two regions ($t(10)=6.44$, $p<.0001$).

Basal-ganglia/frontal/insula vs R TPJ/IFG—When all possible ROI pairings between the basal-ganglia/frontal/insula and R TPJ/IFG networks were averaged, the overall rs-fcMRI between networks was not significant ($t(10)=1.67$, $p>.1$) (Figure 8; see Table 3 and Supplementary Text for regional statistics on pairwise comparisons). Therefore, although both networks were recruited when subjects shifted attention to an unexpected stimulus, they showed at best modest interactions in the resting state.

Dorsal fronto-parietal regions vs basal ganglia/frontal/insula and R TPJ/IFG networks—Because of the primary role of the dorsal network in controlling attention and because dorsal activations for shifts of attention were enhanced when those shifts were unexpected, we measured the resting correlation of the dorsal network with the basal ganglia/frontal/insula and TPJ/IFG networks recruited by unexpected shifts of attention. Average connectivity scores were computed within and between networks (Figure 8). Modest but significant overall positive rs-fcMRI was observed between the basal ganglia/frontal/insula network and dorsal fronto-parietal regions ($t(10)=3.39$, $p=.007$). Pairwise regional analyses indicated that dorsal fronto-parietal rs-fcMRI with the basal ganglia/frontal/insula network was strong through L DLPFC ($t(10) = 6.86$, $p<.0001$; see Supplementary Figure 4) and to a lesser extent L anterior insula ($t(10) = 4.06$, $p=.0023$). Significant connectivity of DLPFC with posterior parietal cortex is consistent with previous anatomical studies in monkeys (Goldman-Rakic, 1988) and functional connectivity studies in humans (Seeley et al., 2007).

In contrast, no significant overall rs-fcMRI was observed between R TPJ-IFG and dorsal frontal-parietal regions ($t(10)=-1.65$, $p > .1$). While this null result could indicate that these regions did not interact during task states, it could also indicate the highly contingent nature of those interactions. We have previously argued that the resting-state independence of R TPJ from both dorsal fronto-parietal and default networks allows TPJ to flexibly switch between those networks during task states (Corbetta et al., 2008).

Eye movement recording

Two summary measures were applied to the eye movement data for each subject. First, the mean eye position during periods in which the left RSVP stream was attended was compared to the mean eye position during periods in which the right RSVP stream was attended, indicating whether there was any overall bias to fixate nearer the attended stream. Second, the mean changes in eye position evoked by stay and shift cues were measured, indicating whether eye movements affected event-related BOLD responses to the cues. In order to compute the second measure, the mean eye position during the 0 msec to 100 msec period following cue onset was used as a baseline while the mean eye position in the 1750 msec to 2000 msec period following cue onset was used to assess movements. Measures in other time periods (e.g. from 550 msec to 775 msec or from 775 to 1000 msec) yielded similar results. Both measures identified two subjects who made excessive movements. For one subject, the mean difference in eye position when the left and right streams were attended was −6.2 deg (where negative numbers refer to a leftward shift), while the mean change in eye position following left and right shift cues was, respectively, −5.3 and 6.5 deg (where negative numbers refer to leftward shifts). For the other subject, the analogous measures were −2.0, −2.4, and 2.0 deg. The data from these two subjects were not included in the results reported above.

For the remaining subjects, the mean difference in eye position when attending to the left and right streams was −0.11 deg. The mean change in eye position following left and right field shift cues was −0.17 deg. and 0.10 deg. respectively. These small deviations in eye position from fixation indicate that subjects largely followed instructions. In addition to the quantitative data given above, each subjects' eyes were carefully monitored via a camera on all scans irrespective of whether eye movement records were also collected.

Finally, our results cannot be explained by eye movements. The regions in TPJ, frontal cortex, insula, and the associative division of the basal ganglia, which provided many of the primary results of the present study, are not classically involved in the control of eye movements. Dorsal fronto-parietal regions do show eye movement responses, but the effects of expectation on reorienting in these regions were actually intermediate between those for TPJ on the one hand and basal ganglia/frontal/insula cortex on the other. Moreover, dorsal parietal regions, as well as occipital regions, showed strong spatially selective attentional activations, which would not have occurred if subjects moved their eyes and fixated the attended stream, and the spatial selectivity of the activations was independent of expectation. Finally, it is unlikely that eye movements occurred during the resting-state scans, in which no peripheral stimuli were presented and the subject's only task was to remain fixated. Yet there was a striking correspondence between the TPJ-IFG and basal ganglia/frontal/insula networks identified from the resting-state scans and the regions identified from the scans involving the RSVP task.

Discussion

Previous work showed that right TPJ and VFC were activated by stimulus-driven reorienting to unexpected stimuli, forming a putative ventral attention network, but did not separately measure effects of reorienting and expectation or identify different functions for these regions (Corbetta and Shulman, 2002). The current results addressed both issues.

Ventral attention network: reorienting and expectation

R TPJ showed a significant difference between stay and shift cues even when they were expected, and this difference was not increased when cues were unexpected and did not depend on visual field. These results suggest that TPJ functioned during stimulus-driven reorienting as a switch or resetting mechanism that was activated in a similar fashion irrespective of the characteristics of the attentional shift. TPJ activity may facilitate transitions of networks between states associated with different environmental stimuli (Corbetta et al., 2008), extending an earlier proposal that TPJ activity (Friedrich et al., 1998) during reorienting 'disengaged' attention (Posner et al., 1984) from the current focus. Additionally, a breach of expectation separately activated TPJ, indicating the critical importance of controlling expectancy effects when studying TPJ. This independent breach of expectation signal may not occur in the same TPJ neurons and/or with the same latency as the reorienting signal.

Both reorienting and expectation signals were consistent with the recent hypothesis that BOLD TPJ activity relates to single-unit activity in the locus coeruleus/norepinephrine (LC/NE) system (Corbetta et al., 2008). The LC/NE system has long been related to changes in arousal (Aston-Jones and Bloom, 1981b, a), a likely consequence of an unexpected event, and the putative role of TPJ in reorienting is similar to recent proposals that LC/NE activity promotes the reorganization of neural networks when a behaviorally important stimulus is detected (Aston-Jones and Cohen, 2005; Bouret and Sara, 2005).

The independence of reorienting and expectation signals strongly dissociated TPJ from the second main component of the ventral attention network, R IFG, which was activated by stimulus-driven reorienting only when reorienting was unexpected. One clue to R IFG function was the relatively weak activation in the present study, in which no motor response was made

to the cue, compared to previous studies that imaged activations to invalid and oddball targets, which involved motor responses. In these latter studies, R IFG activity may have inhibited a prepared response when an unexpected target appeared that potentially required a different course of action (Nobre et al., 1999; Arrington et al., 2000), consistent with the well-documented role of R IFG in response inhibition (Aron et al., 2004a) (although see (Hampshire et al., 2007)).

If R IFG activity inhibits prepared motor responses, why was activity, though weak, observed for an unexpected shift cue not associated with a response? We suggest response-related inhibition may be proactive as well as reactive, i.e. when responses are held in readiness for a target, some inhibition may be generated whenever attention is shifted to an unexpected object. Second, R IFG inhibitory functions may not be purely response-related (Aron et al., 2004a). R TPJ-R IFG co-activation may facilitate termination of ongoing activity and disengagement of attention when shift cues are unexpected.

Both putative inhibitory functions of R IFG activity would lead to strong TPJ-IFG resting-state functional connectivity, since TPJ-IFG co-activation would occur under the ecological conditions in which stimulus-driven reorienting is typically evoked.

A distinct basal ganglia/frontal/insula network

The ventral attention network was distinguished under resting conditions from a second network, comprising bilateral dorsal basal ganglia, anterior cingulate, L DLPFC, and L anterior insula, which was recruited by stimulus-driven shifts of attention only when unexpected. Ventral attention and basal-ganglia/frontal/insula networks may principally involve different neuromodulators, norepinephrine and dopamine, respectively.

Surprisingly, neuroimaging studies of the Posner task, in which a cue indicates the likely location of a subsequent target, have not reported greater basal ganglia activations to targets that occurred in spatially uncued (invalid) than cued (valid) locations (Arrington et al., 2000; Corbetta et al., 2002; Macaluso et al., 2002; Thiel et al., 2004; Kincade et al., 2005; Giessing et al., 2006), even though invalid targets are unexpected, behaviorally relevant, and evoke shifts of attention, while valid targets are expected and do not evoke attentional shifts. Invalid targets in Posner paradigms involving temporal cueing also are not reported to activate basal ganglia (Coull et al., 2000). These null neuroimaging results should be treated very cautiously and may reflect methodological factors, but raise the possibility that the strength of the relationship between breaches of expectation (prediction errors), shifts of attention, and basal ganglia activity depends on the context in which prediction errors/shifts occur, as discussed below.

Animal studies have divided basal ganglia into motor, associative, and limbic divisions (Alexander et al., 1986; Parent and Hazrati, 1995; Middleton and Strick, 2002). The motor division includes a separate oculomotor circuit (Hikosaka and Wurtz, 1983; Hikosaka et al., 1989) that might plausibly be involved in stimulus-driven reorienting (Boussaoud and Kermadi, 1997), particularly given the overlapping brain regions involved in overt and covert orienting (Corbetta et al., 1998). However, the anatomical locations of the most activated basal ganglia region (dorsomedial pallidus) and functionally connected DLPFC/cingulate/insula regions were more consistent with associative than oculomotor pathways. The absence of activity during shifts of attention to middle- or high-probability cues, indicating a predominant influence of cognitive variables, also suggests that basal ganglia activations reflected functions of the associative rather than oculomotor divisions.

The associative division includes lateral prefrontal/basal ganglia circuits (Alexander et al., 1986) that have been implicated in switching between attentional sets (Downes et al., 1993; Owen et al., 1993; Hayes et al., 1998; Monchi et al., 2001; Cools et al., 2004; Cools et al.,

2006). In switching paradigms, a previously irrelevant stimulus/feature is selected to control a behavioral response, updating task-related information in working memory. We suggest that an unexpected stimulus to shift attention evoked a similar updating process. Retrieval/activation in working memory of commands to shift attention (Goldman-Rakic, 1995; Frank et al., 2001; Lewis et al., 2004; Cools et al., 2008; McNab and Klingberg, 2008) may enable unexpected attentional shifts to be implemented by dorsal fronto-parietal regions, perhaps through interactions with L DLPFC (Aron et al., 2004b; Mayr et al., 2006), which showed robust rs-fcMRI with the dorsal network.

The above account leaves open the possibility that basal ganglia/frontal/insula activations during unexpected shifts of attention are more robust in the present than Posner tasks. Prior to an unexpected shift of attention, subjects had not recently shifted attention (present task), rather than just previously on the same trial (Posner), and had been continuously engaged in a demanding monitoring task at the attended location (present task), rather than simply waiting for target onset (Posner). Both features of the present paradigm may have increased the extent to which commands for shifting attention were inactive prior to an unexpected shift stimulus and had to be retrieved/activated.

Switching and spatial attention paradigms have important differences. In task switching paradigms, for example, one of several stimulus-response mappings is executed based on the context provided by other stimuli or instructions, while in spatial attention paradigms shifts of attention are executed that are largely context independent (Hayes et al., 1998). Here, the cue was always a distinctive red square and was always attended. However, fronto-striatal circuits may underlie both context-dependent selection of stimulus-action pairings and selection of less context-dependent but unexpected stimulus-action pairings (peripheral red square->shift attention). Importantly, this putative function of basal ganglia-frontal activity during stimulus-driven reorienting was not exercised routinely, unlike R TPJ, whose activity was closely coupled to reorienting.

The primary role of dorsal fronto-parietal cortex in orienting

During stimulus-driven reorienting to task-relevant objects, TPJ is co-activated with dorsal fronto-parietal regions (present study, (Corbetta et al., 2002; Giessing et al., 2006)). However, when attention is shifted endogenously, only dorsal fronto-parietal regions are activated (Corbetta and Shulman, 2002), indicating their primary role in controlling spatial attention. The precuneus, activated here by stimulus-driven reorienting, is also activated by shifts of attention instructed by symbolic cues at the currently attended location (Yantis et al., 2002).

A clear functional-anatomical segregation was observed between these precuneus ‘shift’ regions (Serences and Yantis, 2006a) and IPS regions that showed sustained spatially-selective signals (Serences and Yantis, 2006b), suggesting complementary roles in shifting and maintaining attention (see (Kelley et al., 2007) and (Molenberghs et al., 2007) for other dissociations). Shift regions may enable spatially-selective sustained regions, which maintain biasing signals in occipital cortex.

Activity in dorsal fronto-parietal shift regions was selectively increased by unexpected shifts of attention, likely reflecting not only increased local activity that specified the parameters of the attentional shift, but also increased interactions with prefrontal regions such as L DLPFC (Goldman-Rakic, 1988; Seeley et al., 2007), which showed significant rs-fcMRI with the dorsal network. Overall, the results in dorsal fronto-parietal regions, i.e. the significant activity observed for expected shifts of attention, the increase in that activity for unexpected shifts, and the presence of spatially-selective modulations, indicated a primary role in shifting spatial attention. The dorsal network, however, was augmented by the ventral network when shifts of

attention were stimulus-driven and by the basal-ganglia/frontal/insula network when infrequent stimulus-driven shifts of attention occurred within a demanding ongoing task.

Supplementary Material

Refer to Web version on PubMed Central for supplementary material.

Acknowledgments

This work was supported by the National Institute of Neurological Disorders and Stroke grant RO1 NS048013, National Institute of Mental Health Grant RO1 MH 71920-06, and the J. S. McDonnell Foundation.

References

Alexander GE, Crutcher MD. Functional architecture of basal ganglia circuits: neural substrates of parallel processing. Trends Neurosci 1990;13:266–271. [PubMed: 1695401]

Alexander GE, Delong MR, Strick PL. Parallel organization of functionally segregated circuits linking basal ganglia and cortex. Annual Review of Neuroscience 1986;9:357–381.

Aron AR, Robbins TW, Poldrack RA. Inhibition and the right inferior frontal cortex. Trends Cogn Sci 2004a;8:170–177. [PubMed: 15050513]

Aron AR, Monsell S, Sahakian BJ, Robbins TW. A componential analysis of task-switching deficits associated with lesions of left and right frontal cortex. Brain 2004b;127:1561–1573. [PubMed: 15090477]

Arrington CM, Carr TH, Mayer AR, Rao SM. Neural mechanisms of visual attention: object-based selection of a region in space. Journal of Cognitive Neuroscience 2000;12:106–117. [PubMed: 11506651]

Aston-Jones G, Bloom FE. Nonrepinephrine-containing locus coeruleus neurons in behaving rats exhibit pronounced responses to non-noxious environmental stimuli. J Neurosci 1981a;1:887–900. [PubMed: 7346593]

Aston-Jones G, Bloom FE. Activity of norepinephrine-containing locus coeruleus neurons in behaving rats anticipates fluctuations in the sleep-waking cycle. J Neurosci 1981b;1:876–886. [PubMed: 7346592]

Aston-Jones G, Cohen JD. An integrative theory of locus coeruleus-norepinephrine function: adaptive gain and optimal performance. Annu Rev Neurosci 2005;28:403–450. [PubMed: 16022602]

Bisley JW, Goldberg ME. Neuronal activity in the lateral intraparietal area and spatial attention. Science 2003;299:81–86. [PubMed: 12511644]

Bouret S, Sara SJ. Network reset: a simplified overarching theory of locus coeruleus noradrenaline function. Trends Neurosci 2005;28:574–582. [PubMed: 16165227]

Boussaoud D, Kermadi I. The primate striatum: neuronal activity in relation to spatial attention versus motor preparation. Eur J Neurosci 1997;9:2152–2168. [PubMed: 9421175]

Boynton GM, Engel SA, Glover GH, Heeger DJ. Linear systems analysis of functional magnetic resonance imaging in human V1. Journal of Neuroscience 1996;16:4207–4221. [PubMed: 8753882]

Brainard DH. The Psychophysics Toolbox. Spatial vision 10(4). 1997

Bressler SL, Tang W, Sylvester CM, Shulman GL, Corbetta M. Top-down control of human visual cortex by frontal and parietal cortex in anticipatory visual spatial attention. J Neurosci 2008;28:10056–10061. [PubMed: 18829963]

Cools R, Clark L, Robbins TW. Differential responses in human striatum and prefrontal cortex to changes in object and rule relevance. J Neurosci 2004;24:1129–1135. [PubMed: 14762131]

Cools R, Ivry RB, D'Esposito M. The human striatum is necessary for responding to changes in stimulus relevance. J Cogn Neurosci 2006;18:1973–1983. [PubMed: 17129185]

Cools R, Gibbs SE, Miyakawa A, Jagust W, D'Esposito M. Working memory capacity predicts dopamine synthesis capacity in the human striatum. J Neurosci 2008;28:1208–1212. [PubMed: 18234898]

Corbetta M, Shulman GL. Control of goal-directed and stimulus-driven attention in the brain. Nat Rev Neurosci 2002;3:201–215. [PubMed: 11994752]

Corbetta M, Kincade JM, Shulman GL. Neural systems for visual orienting and their relationships to spatial working memory. J Cogn Neurosci 2002;14:508–523. [PubMed: 11970810]

Corbetta M, Patel G, Shulman GL. The reorienting system of the human brain: from environment to theory of mind. Neuron 2008;58:306–324. [PubMed: 18466742]

Corbetta M, Miezin FM, Shulman GL, Petersen SE. A PET study of visuospatial attention. Journal of Neuroscience 1993;13:1202–1226. [PubMed: 8441008]

Corbetta M, Kincade JM, Ollinger JM, McAvoy MP, Shulman GL. Voluntary orienting is dissociated from target detection in human posterior parietal cortex. Nature Neuroscience 2000;3:292–297.

Corbetta M, Akbudak E, Conturo TE, Snyder AZ, Ollinger JM, Drury HA, Linenweber MR, Petersen SE, Raichle ME, Van Essen DC, Shulman GL. A common network of functional areas for attention and eye movements. Neuron 1998;21:761–773. [PubMed: 9808463]

Coull JT, Nobre AC. Where and when to pay attention: the neural systems for directing attention to spatial locations and to time intervals as revealed by both PET and fMRI. Journal of Neuroscience 1998;18:7426–7435. [PubMed: 9736662]

Coull JT, Frith CD, Buchel C, Nobre AC. Orienting attention in time: behavioural and neuroanatomical distinction between exogenous and endogenous shifts. Neuropsychologia 2000;38:808–819. [PubMed: 10689056]

de Fockert J, Rees G, Frith CD, Lavie N. Neural correlates of attentional capture in visual search. Journal of Cognitive Neuroscience 2004;16:751–759. [PubMed: 15200703]

Desimone R, Duncan J. Neural mechanisms of selective visual attention. Annu Rev Neurosci 1995;18:193–222. [PubMed: 7605061]

Di Martino A, Scheres A, Margulies DS, Kelly AM, Uddin LQ, Shehzad Z, Biswal B, Walters JR, Castellanos FX, Milham MP. Functional connectivity of human striatum: a resting state FMRI study. Cereb Cortex 2008;18:2735–2747. [PubMed: 18400794]

Dosenbach NU, Visscher KM, Palmer ED, Miezin FM, Wenger KK, Kang HC, Burgund ED, Grimes AL, Schlaggar BL, Petersen SE. A core system for the implementation of task sets. Neuron 2006;50:799–812. [PubMed: 16731517]

Downar J, Crawley AP, Mikulis DJ, Davis KD. The effect of task relevance on the cortical response to changes in visual and auditory stimuli: an event-related fMRI study. Neuroimage 2001;14:1256–1267. [PubMed: 11707082]

Downes JJ, Sharp HM, Costall BM, Sagar HJ, Howe J. Alternating fluency in Parkinson's disease. An evaluation of the attentional control theory of cognitive impairment. Brain 1993;116(Pt 4):887–902. [PubMed: 8353714]

Forman SD, Cohen JD, Fitzgerald M, Eddy WF, Mintun MA, Noll DC. Improved assessment of significant activation in functional magnetic resonance imaging (fMRI): Use of a cluster-size threshold. Magnetic Resonance in Medicine 1995;33:636–647. [PubMed: 7596267]

Fox MD, Corbetta M, Snyder AZ, Vincent JL, Raichle ME. Spontaneous neuronal activity distinguishes human dorsal and ventral attention systems. Proc Natl Acad Sci U S A 2006;103:10046–10051. [PubMed: 16788060]

Frank MJ, Loughry B, O'Reilly RC. Interactions between frontal cortex and basal ganglia in working memory: a computational model. Cogn Affect Behav Neurosci 2001;1:137–160. [PubMed: 12467110]

Friedrich FJ, Egly R, Rafal RD, Beck D. Spatial attention deficits in humans: A comparison of superior parietal and temporal-parietal junction lesions. Neuropsychology 1998;12:193–207. [PubMed: 9556766]

Fuster, JM. The prefrontal cortex. New York: Raven Press; 1989.

Giessing C, Thiel CM, Rosler F, Fink GR. The modulatory effects of nicotine on parietal cortex activity in a cued target detection task depend on cue reliability. Neuroscience 2006;137:853–864. [PubMed: 16309846]

Goldman-Rakic PS. Topography of cognition: Parallel distributed networks in primate association cortex. Annual Review of Neuroscience 1988;11:137–156.

Goldman-Rakic PS. Cellular basis of working memory. Neuron 1995;14:477–485. [PubMed: 7695894]

Hagler DJ Jr, Sereno MI. Spatial maps in frontal and prefrontal cortex. Neuroimage 2006;29:567–577. [PubMed: 16289928]

Hagler DJ Jr, Riecke L, Sereno MI. Parietal and superior frontal visuospatial maps activated by pointing and saccades. Neuroimage 2007;35:1562–1577. [PubMed: 17376706]

Hampshire A, Duncan J, Owen AM. Selective tuning of the blood oxygenation level-dependent response during simple target detection dissociates human frontoparietal subregions. J Neurosci 2007;27:6219–6223. [PubMed: 17553994]

Hayes AE, Davidson MC, Keele SW, Rafal RD. Toward a functional analysis of the basal ganglia. J Cogn Neurosci 1998;10:178–198. [PubMed: 9555106]

He BJ, Snyder AZ, Vincent JL, Epstein A, Shulman GL, Corbetta M. Breakdown of functional connectivity in frontoparietal networks underlies behavioral deficits in spatial neglect. Neuron 2007;53:905–918. [PubMed: 17359924]

Hikosaka O, Wurtz RH. Visual and oculomotor functions of monkey substantia nigra pars reticulata. I. Relation of visual and auditory responses to saccades. Journal of Neurophysiology 1983;49:1230–1253. [PubMed: 6864248]

Hikosaka O, Sakamoto M, Usui S. Functional properties of monkey caudate neurons I. Activities related to saccadic eye movements. Journal of Neurophysiology 1989;61:780–798. [PubMed: 2723720]

Hopfinger JB, Buonocore MH, Mangun GR. The neural mechanisms of top-down attentional control. Nature Neuroscience 2000;3:284–291.

Horvitz JC. Mesolimbocortical and nigrostriatal dopamine responses to salient non-reward events. Neuroscience 2000;96:651–656. [PubMed: 10727783]

Indovina I, Macaluso E. Dissociation of stimulus relevance and saliency factors during shifts of visuospatial attention. Cereb Cortex 2007;17:1701–1711. [PubMed: 17003078]

Jack AI, Patel GH, Astafiev SV, Snyder AZ, Akbudak E, Shulman GL, Corbetta M. Changing human visual field organization from early visual to extra-occipital cortex. PLoS ONE 2007;2:e452. [PubMed: 17505546]

Kastner S, Ungerleider LG. Mechanisms of visual attention in the human cortex. Annu Rev Neurosci 2000;23:315–341. [PubMed: 10845067]

Kastner S, Pinsk MA, De Weerd P, Desimone R, Ungerleider LG. Increased activity in human visual cortex during directed attention in the absence of visual stimulation. Neuron 1999;22:751–761. [PubMed: 10230795]

Kelley TA, Serences JT, Giesbrecht B, Yantis S. Cortical Mechanisms for Shifting and Holding Visuospatial Attention. Cereb Cortex. 2007

Kerr DL, Gusnard DA, Snyder AZ, Raichle ME. Effect of practice on reading performance and brain function. NeuroReport 2004;4:607–610. [PubMed: 15094461]

Kincade JM, Abrams RA, Astafiev SV, Shulman GL, Corbetta M. An event-related functional magnetic resonance imaging study of voluntary and stimulus-driven orienting of attention. The Journal of Neuroscience 2005;25(18):4593–4604. [PubMed: 15872107]

Lewis SJ, Dove A, Robbins TW, Barker RA, Owen AM. Striatal contributions to working memory: a functional magnetic resonance imaging study in humans. Eur J Neurosci 2004;19:755–760. [PubMed: 14984425]

Macaluso E, Frith CD, Driver J. Supramodal effects of covert spatial orienting triggered by visual or tactile events. J Cogn Neurosci 2002;14:389–401. [PubMed: 11970799]

Marois R, Leung HC, Gore JC. A stimulus-driven approach to object identity and location processing in the human brain. Neuron 2000;25:717–728. [PubMed: 10774738]

Mayr U, Diedrichsen J, Ivry R, Keele SW. Dissociating task-set selection from task-set inhibition in the prefrontal cortex. J Cogn Neurosci 2006;18:14–21. [PubMed: 16417679]

McNab F, Klingberg T. Prefrontal cortex and basal ganglia control access to working memory. Nat Neurosci 2008;11:103–107. [PubMed: 18066057]

Middleton FA, Strick PL. Basal-ganglia 'projections' to the prefrontal cortex of the primate. Cereb Cortex 2002;12:926–935. [PubMed: 12183392]

Miller EK, Cohen JD. An integrative theory of prefrontal cortex function. Annu Rev Neurosci 2001;24:167–202. [PubMed: 11283309]

Molenberghs P, Mesulam MM, Peeters R, Vandenberghe RR. Remapping Attentional Priorities: Differential Contribution of Superior Parietal Lobule and Intraparietal Sulcus. Cereb Cortex. 2007

Monchi O, Petrides M, Petre V, Worsley K, Dagher A. Wisconsin Card Sorting revisited: distinct neural circuits participating in different stages of the task identified by event-related functional magnetic resonance imaging. J Neurosci 2001;21:7733–7741. [PubMed: 11567063]

Moore T, Armstrong KM. Selective gating of visual signals by microstimulation of frontal cortex. Nature 2003;421:370–373. [PubMed: 12540901]

Nobre AC, Coull JT, Frith CD, Mesulam MM. Orbitofrontal cortex is activated during breaches of expectation in tasks of visual attention. Nat Neurosci 1999;2:11–12. [PubMed: 10195173]

Nobre AC, Sebestyen GN, Gitelman DR, Mesulam MM, Frackowiack RSJ, Frith CD. Functional localization of the system for visuospatial attention using positron emission tomography. Brain 1997;120:515–533. [PubMed: 9126062]

Ollinger JM, Shulman GL, Corbetta M. Separating Processes within a Trial in Event-Related Functional MRI I. The Method. Neuroimage 2001;13:210–217. [PubMed: 11133323]

Owen AM, Roberts AC, Hodges JR, Summers BA, Polkey CE, Robbins TW. Contrasting mechanisms of impaired attentional set-shifting in patients with frontal lobe damage or Parkinson's disease. Brain 1993;116(Pt 5):1159–1175. [PubMed: 8221053]

Parent A, Hazrati LN. Functional anatomy of the basal ganglia. I. The cortico-basal ganglia-thalamo-cortical loop. Brain Res Brain Res Rev 1995;20:91–127. [PubMed: 7711769]

Pelli DG. The VideoToolbox software for visual psychophysics: transforming numbers into movies. Spatial vision 10(4). 1997

Posner, MI.; Cohen, Y. Components of visual orienting. In: Bouma, H.; Bowhuis, D., editors. Attention and Performance ×. Hillsdale, NJ: Erlbaum; 1984. p. 531-556.

Posner MI, Walker JA, Friedrich FJ, Rafal RD. Effects of parietal injury on covert orienting of attention. Journal of Neuroscience 1984;4:1863–1874. [PubMed: 6737043]

Postuma RB, Dagher A. Basal ganglia functional connectivity based on a meta-analysis of 126 positron emission tomography and functional magnetic resonance imaging publications. Cereb Cortex 2006;16:1508–1521. [PubMed: 16373457]

Prodoehl J, Yu H, Little DM, Abraham I, Vaillancourt DE. Region of interest template for the human basal ganglia: comparing EPI and standardized space approaches. Neuroimage 2008;39:956–965. [PubMed: 17988895]

Redgrave P, Prescott TJ, Gurney K. Is the short-latency dopamine response too short to signal reward error? Trends Neurosci 1999a;22:146–151. [PubMed: 10203849]

Redgrave P, Prescott TJ, Gurney K. The basal ganglia: a vertebrate solution to the selection problem? Neuroscience 1999b;89:1009–1023. [PubMed: 10362291]

Ruff CC, Blankenburg F, Bjoertomt O, Bestmann S, Freeman E, Haynes J-D, Rees G, Josephs O, Deichmann R, Driver J. Concurrent TMS-fMRI and Psychophysics Reveal Frontal Influences on Human Retinotopic Visual Cortex. Current Biology 2006;16:1479–1488. [PubMed: 16890523]

Saygin AP, Sereno MI. Retinotopy and attention in human occipital, temporal, parietal, and frontal cortex. Cereb Cortex 2008;18:2158–2168. [PubMed: 18234687]

Schluppeck D, Glimcher P, Heeger DJ. Topographic organization for delayed saccades in human posterior parietal cortex. J Neurophysiol 2005;94:1372–1384. [PubMed: 15817644]

Schultz W. Predictive reward signal of dopamine neurons. J Neurophysiol 1998;80:1–27. [PubMed: 9658025]

Seeley WW, Menon V, Schatzberg AF, Keller J, Glover GH, Kenna H, Reiss AL, Greicius MD. Dissociable intrinsic connectivity networks for salience processing and executive control. J Neurosci 2007;27:2349–2356. [PubMed: 17329432]

Serences JT, Yantis S. Selective visual attention and perceptual coherence. Trends Cogn Sci 2006a; 10:38–45. [PubMed: 16318922]

Serences JT, Yantis S. Spatially Selective Representations of Voluntary and Stimulus-Driven Attentional Priority in Human Occipital, Parietal, and Frontal Cortex. Cereb Cortex. 2006b

Serences JT, Shomstein S, Leber AB, Golay X, Egeth HE, Yantis S. Coordination of voluntary and stimulus-driven attentional control in human cortex. Psychol Sci 2005;16:114–122. [PubMed: 15686577]

Sereno MI, Pitzalis S, Martinez A. Mapping of contralateral space in retinotopic coordinates by a parietal cortical area in humans. Science 2001;294:1350–1354. [PubMed: 11701930]

Silver MA, Ress D, Heeger DJ. Topographic maps of visual spatial attention in human parietal cortex. J Neurophysiol 2005;94:1358–1371. [PubMed: 15817643]

Swisher JD, Halko MA, Merabet LB, McMains SA, Somers DC. Visual topography of human intraparietal sulcus. J Neurosci 2007;27:5326–5337. [PubMed: 17507555]

Sylvester CM, Shulman GL, Jack AI, Corbetta M. Asymmetry of anticipatory activity in visual cortex predicts the locus of attention and perception. Journal of Neuroscience. 2007

Talairach, J.; Tournoux, P. New York: Thieme Medical Publishers, Inc.; 1988. Co-Planar Stereotaxic Atlas of the Human Brain.

Thiel CM, Zilles K, Fink GR. Cerebral correlates of alerting, orienting and reorienting of visuospatial attention: an event-related fMRI study. Neuroimage 2004;21:318–328. [PubMed: 14741670]

Van Essen DC. A Population-Average, Landmark- and Surface-based (PALS) atlas of human cerebral cortex. Neuroimage 2005;28:635–662. [PubMed: 16172003]

Vandenberghe R, Duncan J, Dupont P, Ward R, Poline J-B, Bormans G, Michiels J, Mortelmans L, Orban GA. Attention to one or two features in left and right visual field: a positron emission tomography study. Journal of Neuroscience 1997;17:3739–3750. [PubMed: 9133394]

Yantis S, Schwarzbach J, Serences J, Carlson RL, Steinmetz MA, Pekar JJ, Courtney SM. transient neural activity in human parietal cortex during spatial attention shifts. Nature Neuroscience 2002;5:995–1002.

Zink CF, Pagnoni G, Martin ME, Dhamala M, Berns GS. Human striatal response to salient nonrewarding stimuli. J Neurosci 2003;23:8092–8097. [PubMed: 12954871]

Zink CF, Pagnoni G, Chappelow J, Martin-Skurski M, Berns GS. Human striatal activation reflects degree of stimulus saliency. Neuroimage 2006;29:977–983. [PubMed: 16153860]

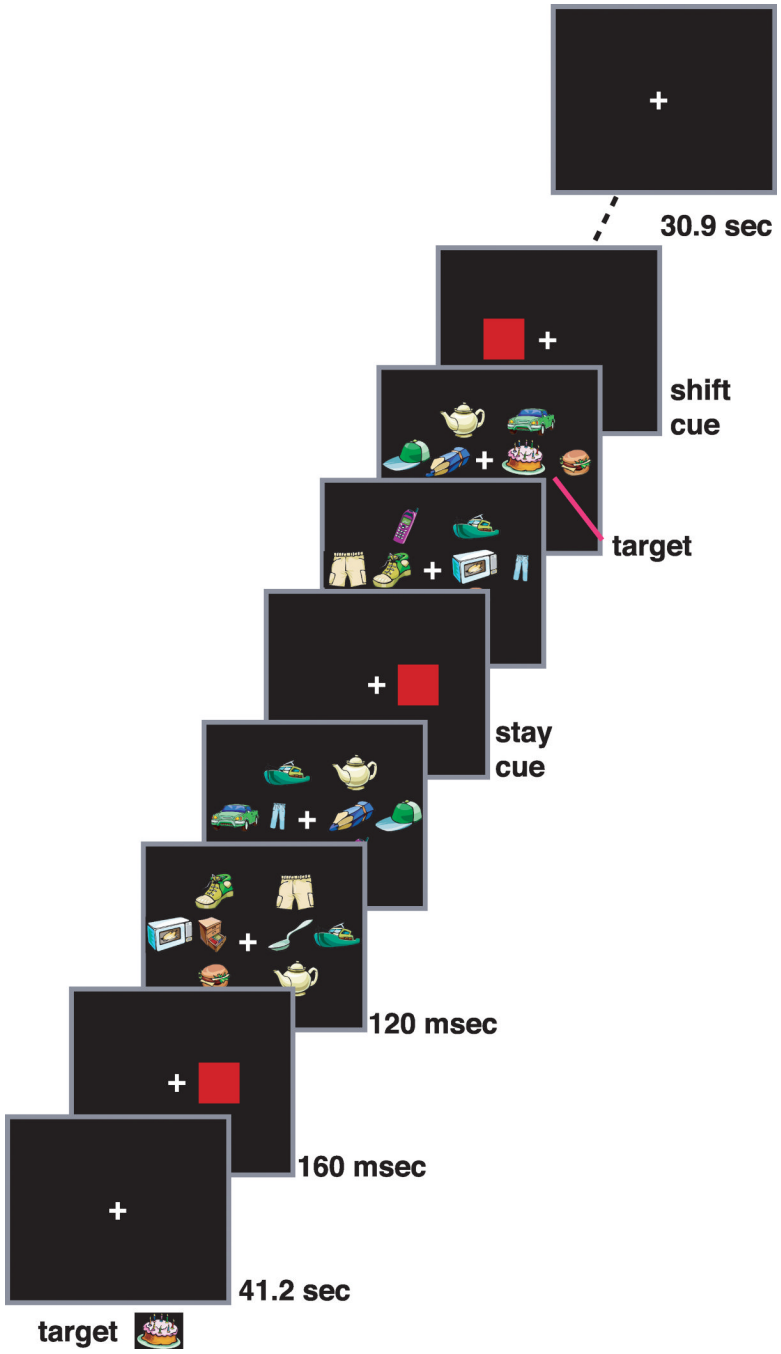

Figure 1.
Procedure. The target object to be detected was presented at the beginning of the scan. Following a fixation period (41.2 sec), a red square (160 msec duration) cue indicated the RSVP stream in which targets would appear. Subsequent cues indicated targets would continue to appear in the currently attended stream (stay cues) or would appear in the opposite stream (shift cues). Successive cues were separated by 2.06, 4.12, or 6.18 secs while successive targets were separated on average by 10.5 sec. The scan ended following a post-task fixation period (30.9 sec). Across scans, the probability of a shift vs stay cue was varied to manipulate expectation. See text for details.

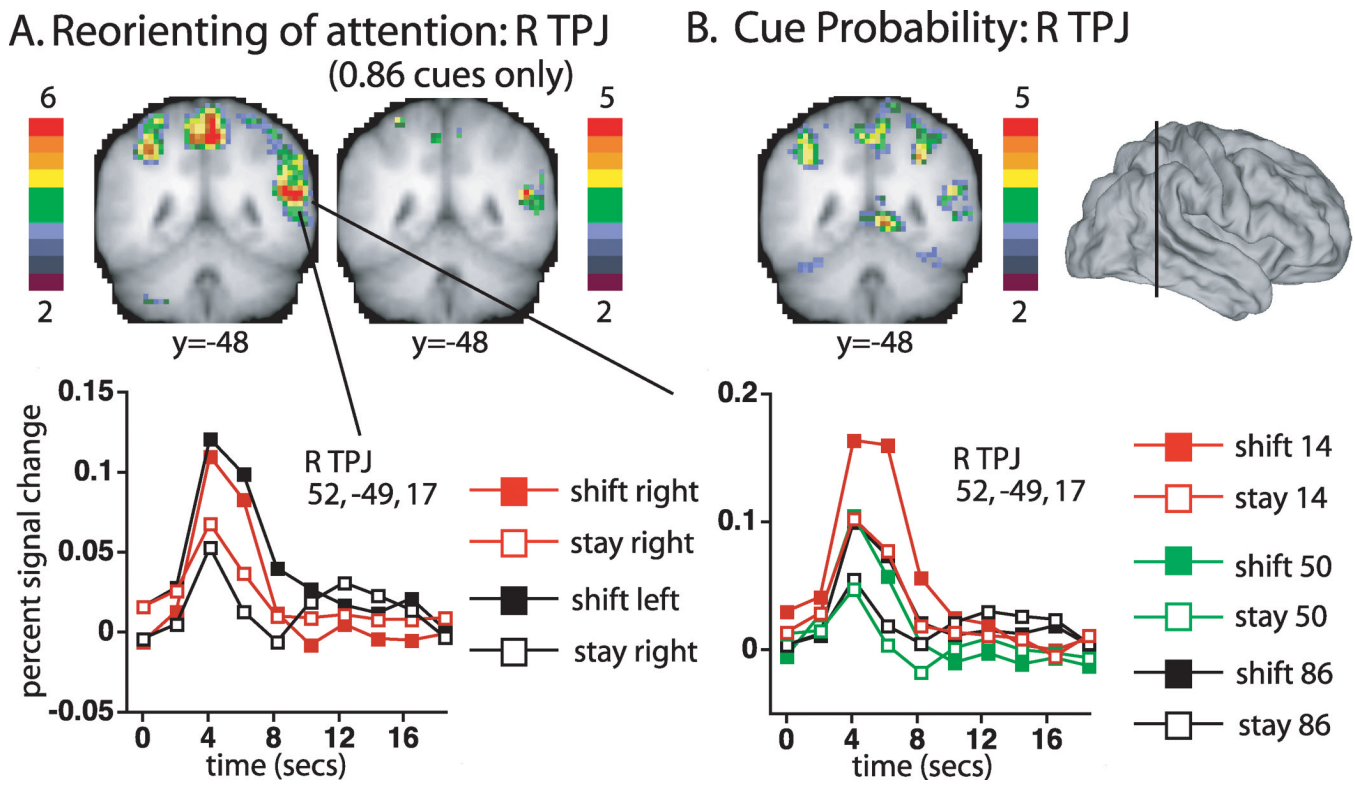

Figure 2.

A) The left coronal slice shows voxels that showed significant differences between shift and stay cues (from the group Cue Type by Time ANOVA map, corrected for multiple comparisons). The color bar indicates the equivalent z-score for the p-value from the ANOVA. The right coronal slice shows the corrected voxel-wise map when only high probability (0.86) stay and shift conditions were included. The graphs show the timecourse of activation in the R TPJ ROI defined from the Cue Type by Time map, as a function of Cue Type and Cue Location (left graph), or Cue Type and Cue Probability (right graph). B) Voxels that showed a significant effect of Cue Probability (coronal slice from the group Cue Probability (0.86, 0.50, 0.14) by Time ANOVA map, corrected for multiple comparisons). The line through the lateral surface view indicates the position of the coronal slice y=−48. R=right; TPJ=temporo-parietal junction.

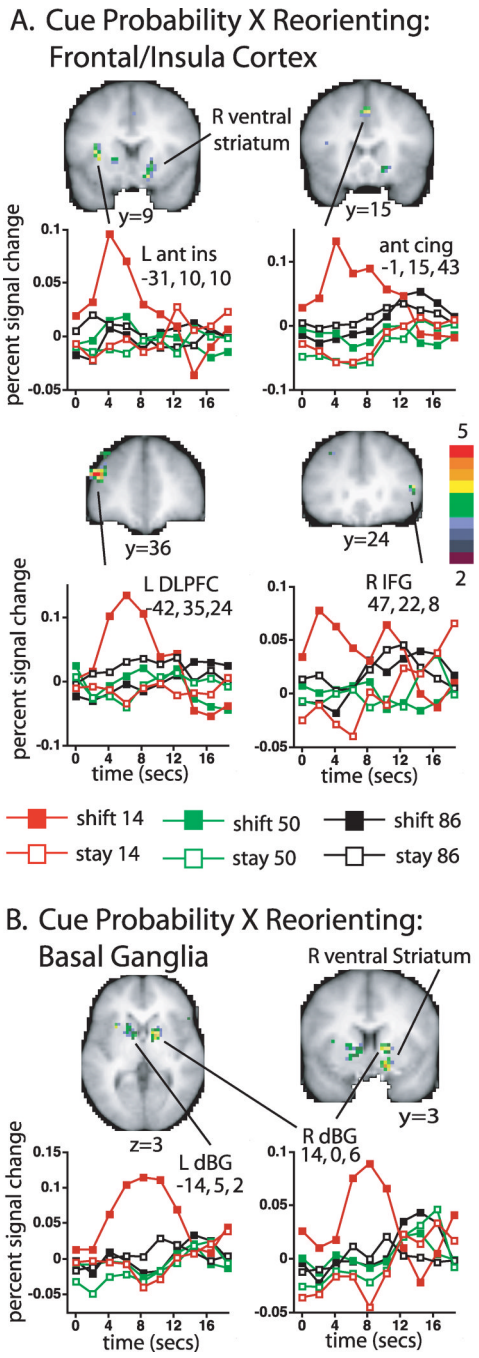

Figure 3.

Voxels in insula and frontal cortex (A) and basal ganglia (B) that showed a significant interaction of the shift vs. stay effect with Cue Probability (transverse and coronal slices from the group Cue Type by Cue Probability by Time ANOVA map, corrected for multiple comparisons). While the location of the most strongly activated voxels in the dorsal basal ganglia and the Talairach coordinates assigned to the dorsal activation foci by our automatic peak-finding procedure were most consistent with a globus pallidus assignment (Prodoehl et al., 2008), adjacent parts of the caudate were also activated, as shown in the slices. The color bar indicates the equivalent z-score for the p-value from the ANOVA. The graphs show the timecourse of the BOLD signal as a function of Cue Type and Cue Probability. Ant ins =

anterior insula; ant cing = anterior cingulate; DLPFC = dorsolateral prefrontal cortex; IFG=inferior frontal gyrus; dBG = dorsal basal ganglia; L=left; R=right.

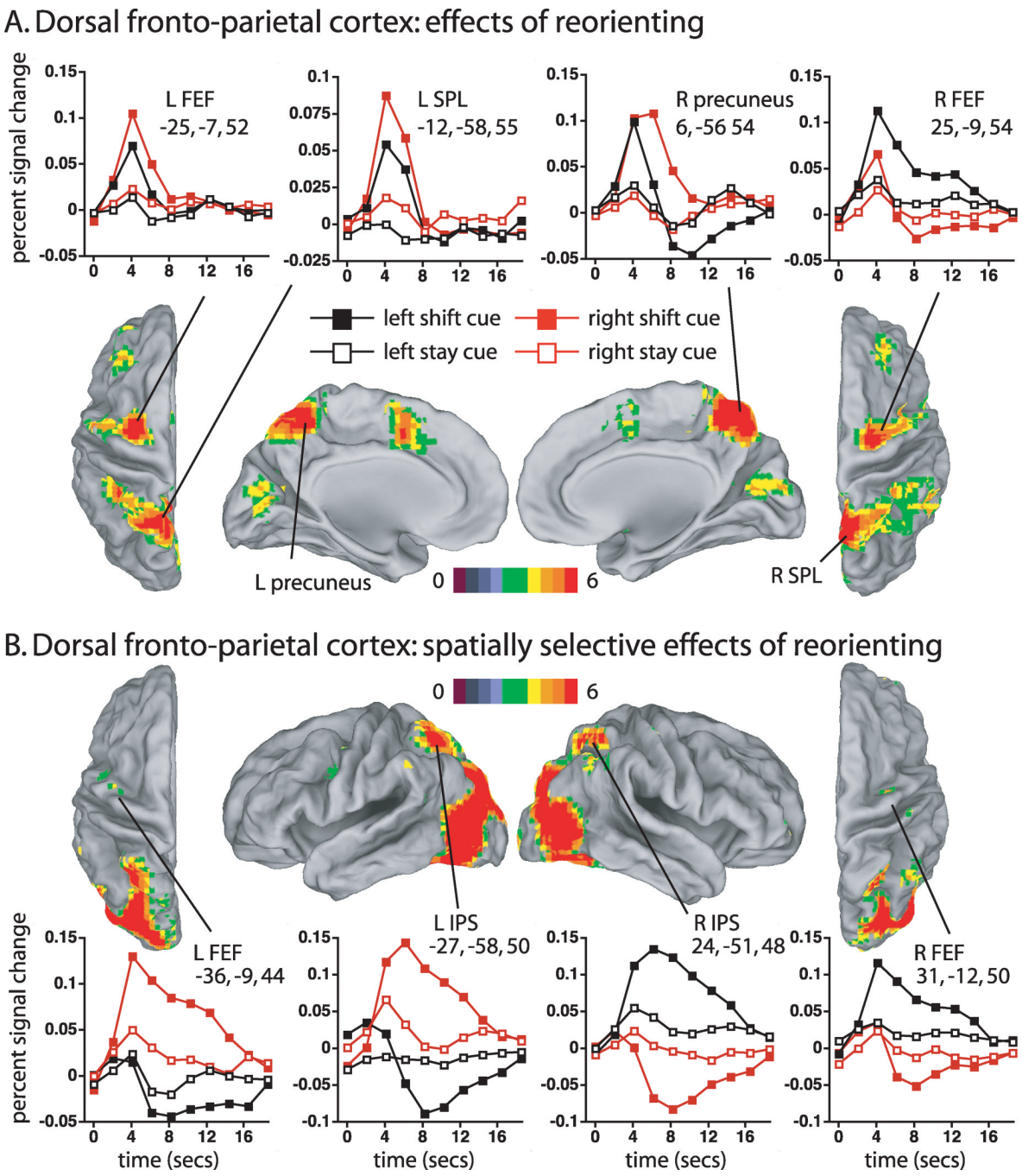

Figure 4.

A) Dorsal and medial views of voxels that showed significantly different activations following shift and stay cues (Cue Type by Time ANOVA map, corrected for multiple comparisons). The graphs show the timecourse of the BOLD signal as a function of Cue Type and Cue Location. The color bar indicates the equivalent z-score for the p-value from the ANOVA. B) Dorsal and lateral views of voxels in which the difference between shift and stay cues significantly depended on the location of the cue (Cue Location by Cue Type by Time, corrected for multiple comparisons). L=left; R=right; SPL=superior parietal lobule; IPS=intraparietal sulcus; FEF=frontal eye fields. PrCs=precentral sulcus.

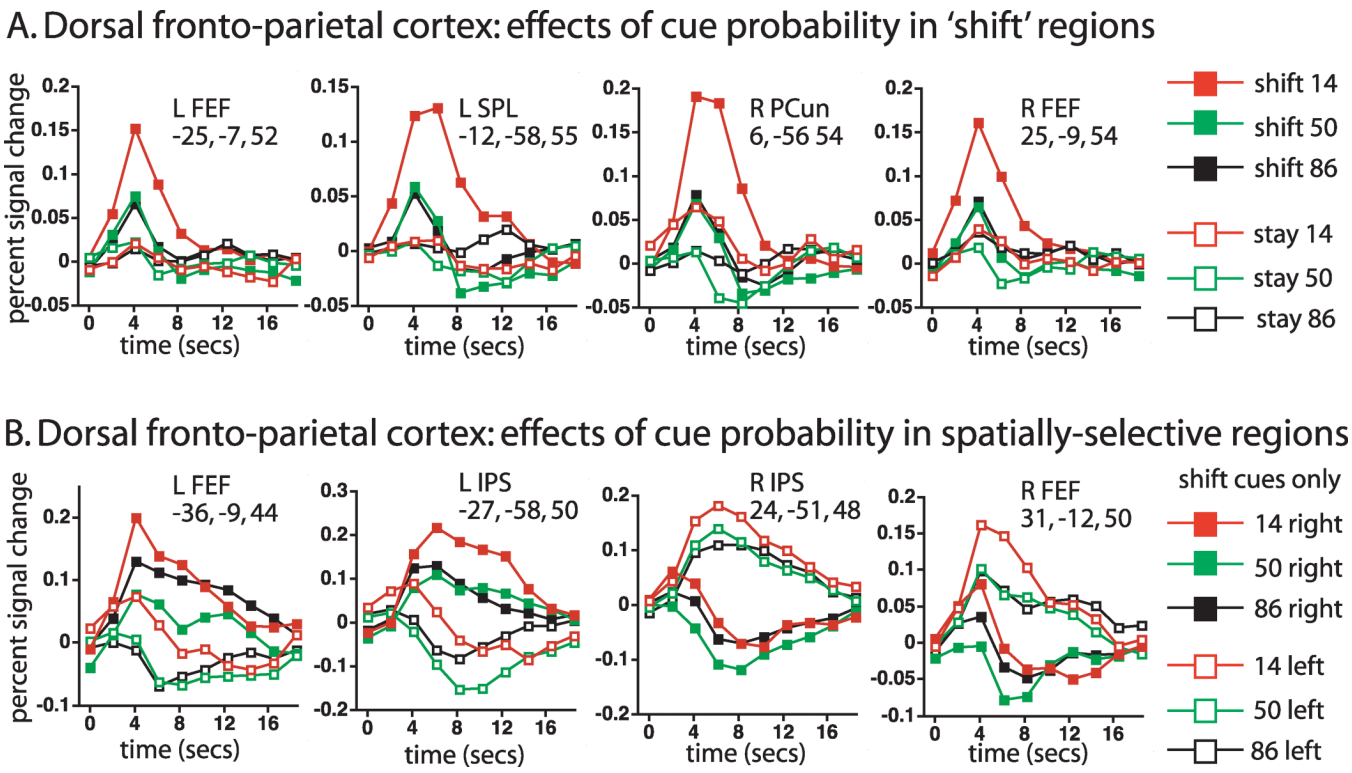

Figure 5.

A) The graphs show the timecourse of the BOLD signal as a function of Cue Type and Cue Probability in ROIs defined from the Cue Type by Time map, corrected for multiple comparisons. B) The graphs show the timecourse of the BOLD signal for shift cues only as a function of Cue Probability and Cue Location in ROIs defined by the Cue Type by Cue Location by Time map, corrected for multiple comparisons. L=left; R=right; PCun=precuneus; SPL=superior parietal lobule; IPS=intraparietal sulcus; FEF=frontal eye fields.

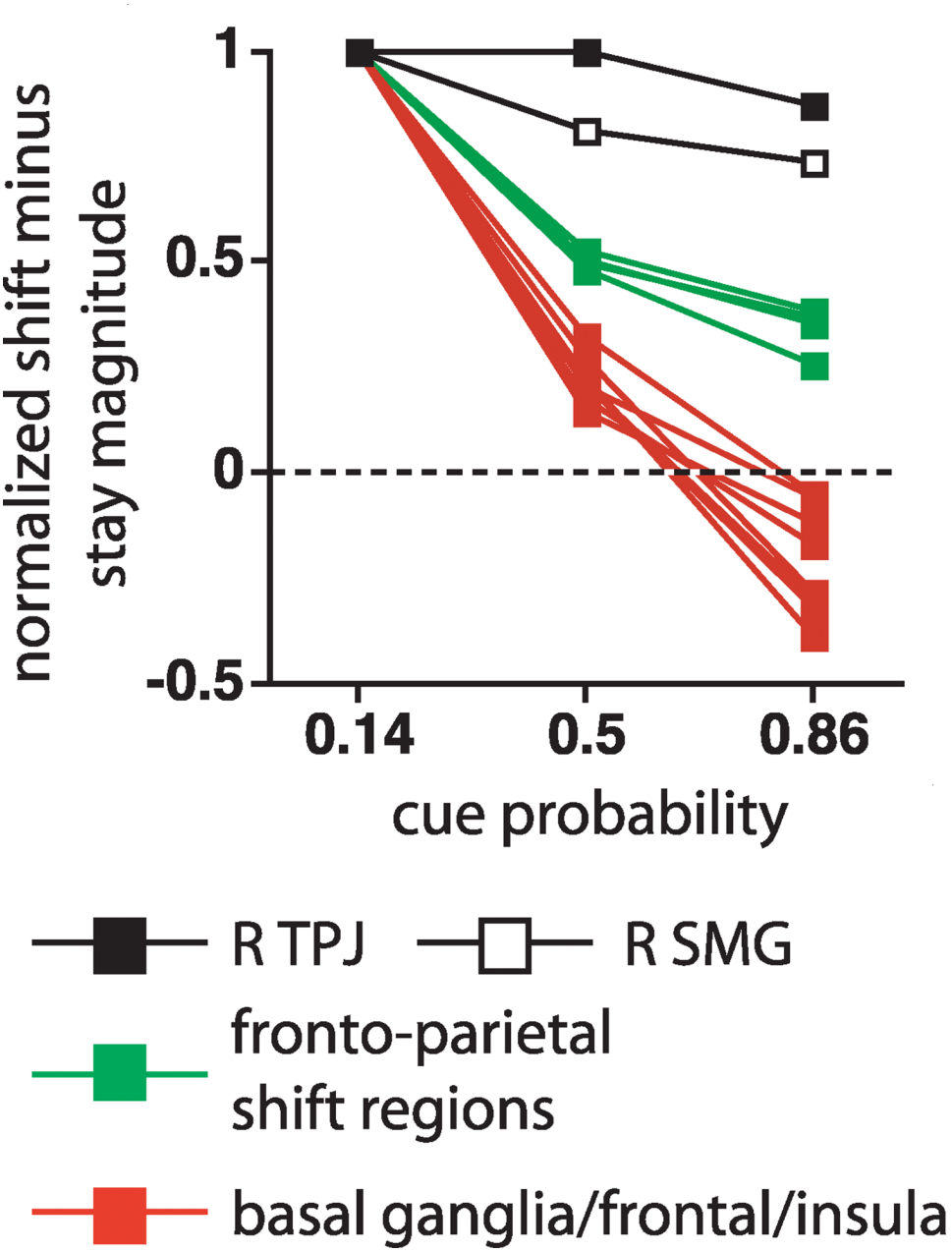

Figure 6.

The graphs display the shift cue minus stay cue magnitude at three probability levels, normalized by the magnitude at the 0.14 probability level. Each line in the graph corresponds to a different ROI. The R TPJ and R SMG ROIs are taken from the multiple-comparison corrected Cue Type by Time ANOVA map. The fronto-parietal 'shift' ROIs are the 4 foci that showed the largest z-scores in the multiple-comparison corrected Cue Type by Time map (Table 2), and the 8 basal ganglia/frontal/insula ROIs are from the multiple-comparison corrected Cue Type by Cue Probability by Time map (Table 1).

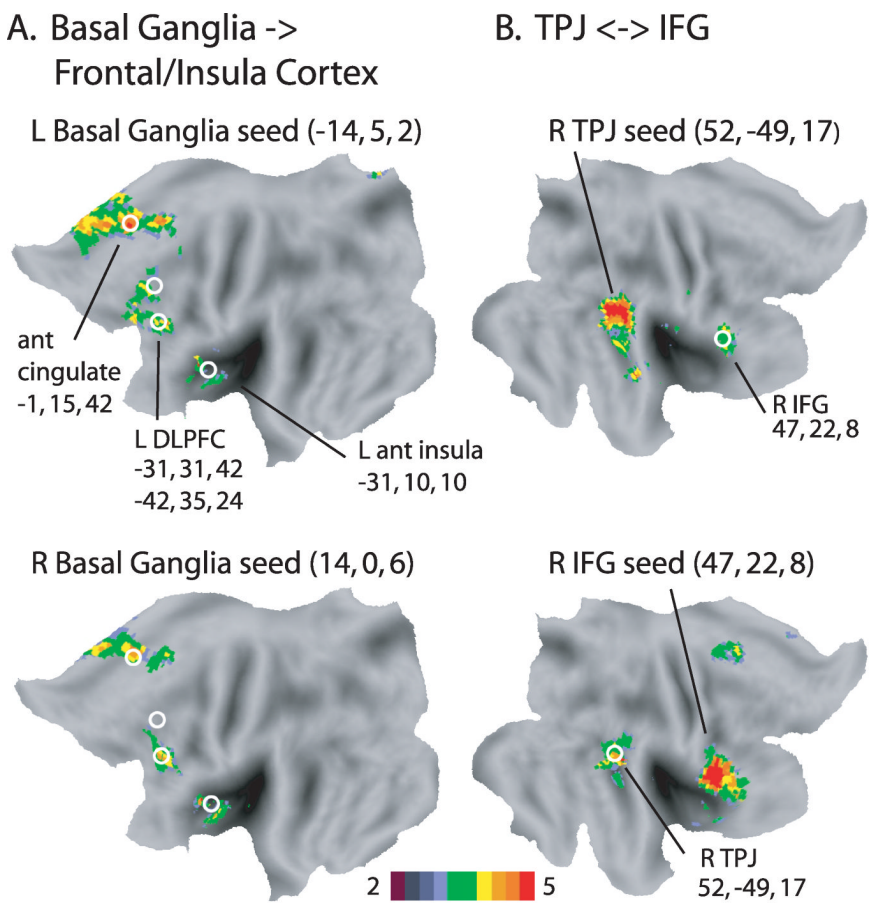

Figure 7.

A) Flat-maps of voxel-wise rs-fcMRI statistical maps in a separate group of subjects (n=11) using as seeds the left and right dorsal basal ganglia ROIs that showed a significant interaction of Cue Type by Cue Probability by Time, corrected for multiple comparisons. The group voxel-wise z-map is shown for a 1-sample, random effects t-test, corrected for multiple comparisons, of whether the Fisher z-transformed correlation values were different from zero. The white circles indicate the location of the frontal and anterior insula foci that showed a significant Cue Type by Cue Probability by Time interaction, corrected for multiple comparisons, during the scans involving the RSVP task. B) Flat-maps of voxel-wise rs-fcMRI between R TPJ and R IFG. The group voxel-wise z-map is shown for a 1-sample, random effects t-test, corrected for multiple comparisons, of whether the Fisher z-transformed correlation values were different from zero. In the top map, the seed was centered at the significant R TPJ focus that showed different timecourses for stay and shift cues during the RSVP task (i.e. Figure 2A, Cue Type by Time ANOVA map, corrected for multiple comparisons), while in the bottom map, the seed was centered at the significant R IFG focus from the interaction map (i.e. Cue Type by Cue Probability by Time, corrected for multiple comparisons) for the RSVP task. TPJ=temporo-parietal junction; IFG=inferior frontal gyrus; DLPFC = dorsolateral prefrontal cortex; ant=anterior.

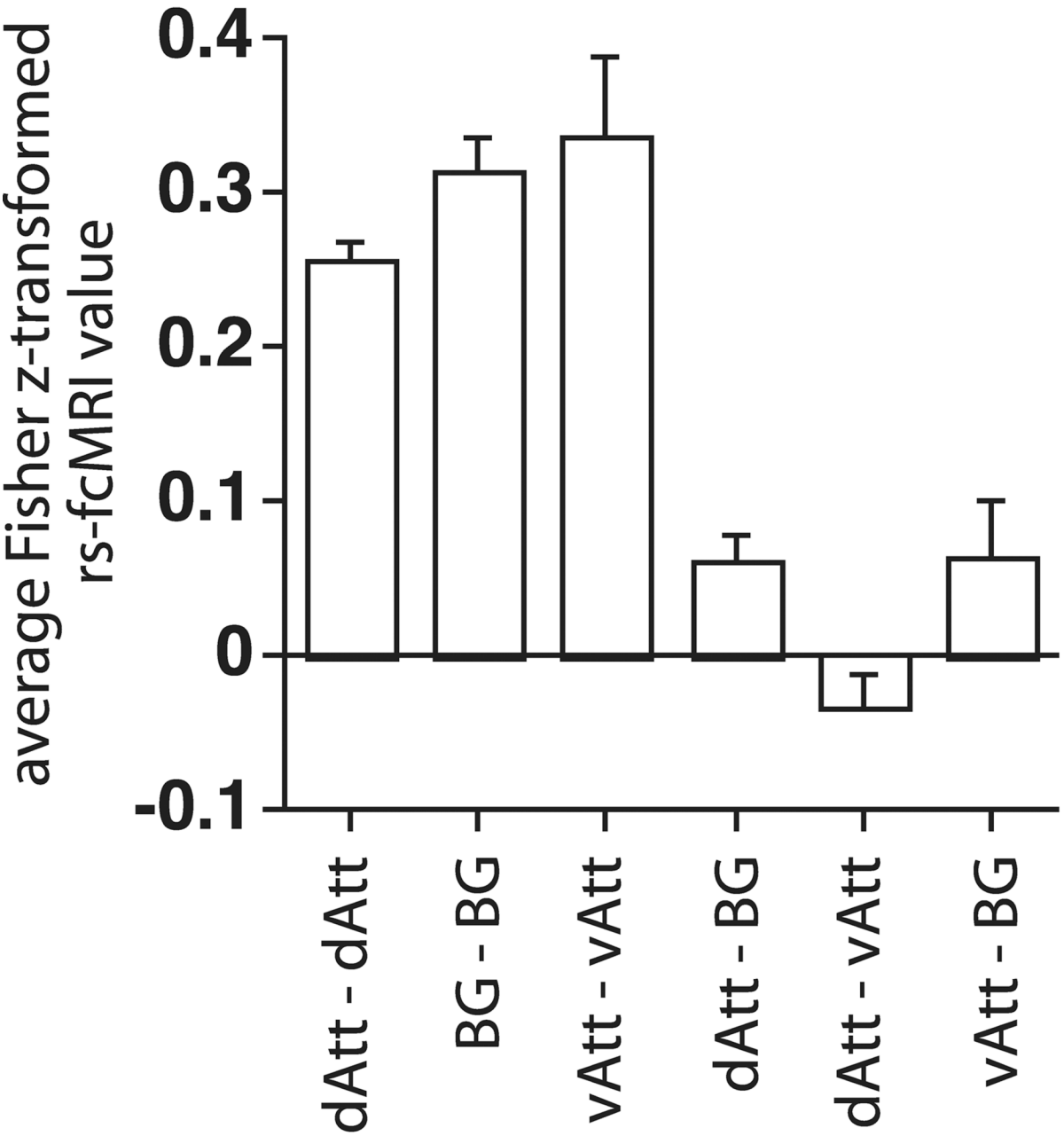

Figure 8.

The graph shows the group-averaged Fisher z-transformed value for all ROI pairs within a network for three different networks, or for all ROI pairs between networks. Error bars are computed over the 11 subjects. dAtt = the dorsal attention network, comprising 35 regions (see Table 2 for all foci): 18 foci that showed a shift vs stay difference (from the Cue Type by Time map, corrected for multiple comparisons), 11 foci that showed a shift vs stay difference that depended on cue location (from the Cue Type by Cue Location by Time map, corrected for multiple comparisons), and 6 foci that showed a shift vs stay difference that depended on cue probability (from the Cue Type by Cue Probability by Time map, corrected for multiple comparisons). BG = the basal ganglia/frontal/insula network, comprising 5 regions: L and R

dorsal basal ganglia, anterior cingulate, L DLPFC, and L anterior insula. vAtt = the ventral attention network, comprising R TPJ and R IFG.

Table 1

TPJ, SMG, Prefrontal, anterior insular, and basal ganglia regions that showed significant differences between stay and shift cues in voxel-wise statistical maps, corrected for multiple comparisons

Region	x	y	z	z-score	Region	x	y	z	z-score
CueType (shift, stay) × Time					CueType (shift, stay) × CueProbability (0.14, 0.50, 0.86) × Time				
R TPJ	52	−49	17	6.45	anterior cingulate	−1	15	43	4.44
R SMG	51	−45	32	5.60	L anterior insula	−31	10	10	4.12
					R IFG	47	22	8	3.81
anterior cingulate	−4	8	46	5.41	L DLPFC	−42	35	24	5.21
	4	18	37	3.17		−31	32	42	3.77
L anterior insula	−29	11	13	5.11					
L IFG	−31	47	14	3.89	L dorsal basal ganglia	−14	5	2	3.89
R IFG	48	14	10	4.32	R dorsal basal ganglia	14	0	6	4.61
	36	17	16	3.66	R ventral striatum	15	6	−10	4.62
L DLPFC	−42	36	22	4.06					
	−33	32	31	5.02					
R DLPFC	28	33	33	4.01					
	30	42	23	3.96					
R basal ganglia	13	4	−6	3.71					
	15	−2	20	3.33					

Table 2

Dorsal frontal-parietal regions that showed significant differences between stay and shift cues in voxel-wise statistical maps, corrected for multiple comparisons

Region	x	y	z	z-score	Region	x	y	z	z-score
CueType (shift, stay) × Time					CueType (shift, stay) × CueLocation (left, right) × Time				
L Precuneus/SPL	−12	−58	55	7.19	L SPL	−7	−71	52	3.82
L SPL	−15	−69	46	5.25	L SPL/IPS	−16	−80	42	5.59
R Precuneus	6	−56	54	7.44	L IPS	−27	−58	50	7.59
R SPL/Precuneus	6	−71	56	4.11	L ventral IPS	−25	−75	30	8.75
L ant IPS	−33	−46	57	4.50	R SPL/IPS	15	−85	39	5.08
L IPS	−28	−54	44	4.60	R IPS	24	−51	48	8.78
R IPS	27	−48	61	4.84	R ventral IPS	26	−82	32	7.38
	33	−56	52	3.94	L ventral Precentral	−41	2	33	4.12
	21	−62	39	3.59	L Precentral	−49	−4	52	4.66
L Postcentral	−35	−41	43	6.03	L FEF	−36	−9	44	4.13
R dorsal SMG	37	−41	49	4.59	R FEF	31	−12	51	4.78
R dorsal SMG	42	−57	43	3.64					
L FEF	−25	−7	52	7.30	CueType (shift, stay) × CueProbability (0.14, 0.50, 0.86) × Time				
R FEF	25	−9	54	6.96	L SPL	−7	−69	53	5.31
L Precentral	−48	−4	39	5.02	R SPL	11	−67	57	5.22
	−36	2	32	3.23	L ant IPS	−30	−49	40	4.74
R Precentral	43	2	40	4.91	L Precuneus	−4	−57	49	4.15
SMA	−1	0	56	4.76	R FEF	22	−9	61	4.49
					R FEF	39	−14	48	4.38

J Neurosci. Author manuscript; available in PMC 2010 April 8.

Table 3

p-values of resting-state fcMRI between indicated regions.

	L dBG	R dBG	ant cing	L ant ins	L DLPFC	R IFG	R TPJ
L dBG		+++	+++	+	++	--	--
R dBG			+++	++	+++	−	--
ant cing				+++	+++	+	--
L ant ins					+++	+	--
L DLPFC						--	--
R IFG							+++
R TPJ							

+++ = p <.005

++ = p <.01

+ = p <.05

− = p<0.1

-- = p >.1

dBG=dorsal basal ganglia, ant=anterior; L=left; cing=cingulate; ins=insula
DLPFC=dorsolateral prefrontal cortex
R=right; IFG=inferior frontal gyrus; TPJ=temporo-parietal junction